

An Effective Resource-Competition Model for Species Coexistence

Deepak Gupta^{1,2,*}, Stefano Garlaschi^{1,*}, Samir Suweis¹, Sandro Azaele¹, and Amos Maritan¹

¹*Dipartimento di Fisica e Astronomia “Galileo Galilei”,*

Università degli Studi di Padova, via Marzolo 8, 35131 Padova, Italy and

²*Department of Physics, Simon Fraser University, Burnaby, British Columbia V5A1S6, Canada*

(Dated: March 25, 2022)

Local coexistence of species in large ecosystems is traditionally explained within the broad framework of niche theory. However, its rationale hardly justifies rich biodiversity observed in nearly homogeneous environments. Here we consider a consumer-resource model in which effective spatial effects, induced by a coarse-graining procedure, exhibit stabilization of intra-species competition. We find that such interactions are crucial to maintain biodiversity. Herein, we provide conditions for several species to live in an environment with a very few resources. In fact, the model displays two different phases depending on whether the number of surviving species is larger or smaller than the number of resources. We obtain conditions whereby a species can successfully colonize a pool of coexisting species. Finally, we analytically compute the distribution of the population sizes of coexisting species. Numerical simulations as well as empirical distributions of population sizes support our analytical findings.

Our planet hosts an enormous number of species [1], which thrive within a variety of environmental conditions. The coexistence of this enormous biological diversity is traditionally explained in terms of local adaptation [2, 3], environmental heterogeneity [4, 5], species’ abilities to aptly respond to the distribution of resources [6, 7], and other abiotic factors which broadly define a niche [8]. When species are geographically separated, they may survive because they match a specific environmental condition and inter-specific competition is not detrimental. However, several microbial species seem to coexist despite they occupy very similar niches in close-by regions [9–11]. This scenario is known as the *paradox of plankton* [12]. Now, on timescales that are larger than one generation but smaller than speciation timescales, the fittest species should outcompete all the others. Then, why do we still observe coexistence? Consistent with this rationale, theoretical work based on MacArthur’s *consumer-resource model* [13, 14] confirms the validity of the so called *competitive exclusion principle* (CEP): the number of coexisting species competing for the same resources is bounded by the number of resources themselves [15–21]. Such a stark contrast between the predictions of CEP and coexistence of many species has been resolved by incorporating metabolic trade-off [22], adaptive metabolic strategies [23, 24], enrichment of resources [25] and multiple stable states [26]. Finally, consumer-resource models are well suited to investigate how interactions reverberate on coexistence, but it is usually hard to calculate community patterns which we more easily observe.

A complementary framework, which has been able to explain several biodiversity patterns at macroscopic scales, is the neutral theory of biogeography [27–34]. Instead of looking at what specific traits facilitate species’ survival, this approach highlights the general features which tend to make species more similar to each other. This framework has the merit to predict several patterns

in agreement with the empirical data [35–40]. However, it lacks a convincing mechanism of coexistence, which is usually maintained only by an external source of individuals. Within this context, competition for resources plays a relatively minor role with respect to the niche setting, and the total number of species sustained by a region cannot be inferred by the availability of resources in the habitat. Finally, because species are competitively equivalent, and therefore, they lack any specific identity, it is difficult to explain whether an individual is successful in invading an ecosystem made of coexisting species.

In this Letter, we propose an alternative approach based on a generalization of the aforementioned MacArthur’s consumer-resource model. This new formulation explains why a large number of species can coexist even in the presence of a limited number of resources, thus violating CEP. Secondly, it predicts how many species will survive depending on the amount of resource present in the habitat. Thirdly, we find the conditions under which an invading species outcompetes a pool of coexisting species. Finally, we analytically obtain the species abundance distribution (SAD), i.e., the probability distribution of the population sizes of the species, and show that it justifies the empirical SAD calculated from the plankton data presented in Ref. [41].

The key feature of this new framework is the effect of a stabilizing intra-species interaction term, which affects the dynamics on top of the traditional inter-species interaction terms which account for the indirect resource consumption. This stabilizing factor emerges naturally in all ecosystems when spatial effects are not negligible. Indeed, by introducing a coarse-graining of the spatial degrees of freedom, we show that a density-dependent inhibition term emerges, which stabilizes the dynamics through a carrying capacity term (see full derivation in the supplementary material [42]). For example in tree communities, such density-dependent term may model

Janzen-Connell effect (JCE) [43–45], that describes the inhospitability for the seedlings in the proximity of parent trees due to host-specific pathogens. This results in penalization of their growth and it inhibits the local crowding of individuals belonging to the same species [46–48].

To begin with, we consider an ecological community composed of M different species competing for R resources. These species are characterized by their maximum consumption rates, $\alpha_{\sigma i}$, at which a species σ uptakes the i -th resource and converts it into its biomass at high concentration of the resource, c_i . In what follows, we also refer to the α 's as *metabolic strategies*. Since per-capita growth rates are proportional to the resource concentrations when they are low, the overall dependence of resource concentration is typically captured by multiplying the maximum growth rate by the *Monod function*, $r_i(c_i) = c_i/(k_i + c_i)$, where k_i is a resource dependent constant. Further, resources degrade in time with a rate μ_i . Similarly, populations decay with intrinsic mortality rate β_σ . Therefore, the system evolves with an extended consumer-resource model [13, 14]:

$$\dot{n}_\sigma = n_\sigma \left[\sum_{i=1}^R \alpha_{\sigma i} r_i(c_i) - \beta_\sigma - \epsilon_\sigma n_\sigma \right], \quad (1)$$

$$\dot{c}_i = \mu_i(\Lambda_i - c_i) - r_i(c_i) \sum_{\sigma=1}^M n_\sigma \alpha_{\sigma i}, \quad (2)$$

where we have included an additional contribution $\epsilon_\sigma n_\sigma^2$ in Eq. (1) that corresponds to intra-species interactions. Herein, ϵ_σ^{-1} may be treated as proportional to the carrying capacity for the species σ . In Eq. (2), the quantity $\mu_i \Lambda_i$ is the rate of supplying *abiotic* resources. Notice that biotic resources are typically modeled by substituting μ_i with $\mu_i c_i$. Then, $\mu_i \Lambda_i$ and Λ_i , respectively, correspond to the growth rate and the carrying capacity of the i -th resource. In what follows, for simplicity, we report the results for the case of abiotic resources with degradation rates of all resources to be the same: $\mu = \mu_i$. The other cases do not display qualitatively different results.

As the time progresses, we expect the system to reach a stationary state. If all the species have survived at a large-time, then the following equations in the matrix form can be obtained by setting the left-hand side (LHS) of Eqs. (1) and (2) equal to zero:

$$\vec{\mathcal{N}} = E^{-1}(QG \vec{\mathcal{U}} - \vec{\mathcal{B}}), \quad (3)$$

$$\mu(\vec{\mathcal{L}} - \vec{\mathcal{X}}) = GQ^T \vec{\mathcal{N}}, \quad (4)$$

where Q is a $M \times R$ matrix whose elements are the metabolic strategies ($[Q]_{\sigma i} = \alpha_{\sigma i}$), $G = \text{diag}[r_1(c_1^*), r_2(c_2^*), \dots, r_R(c_R^*)]$, $E = \text{diag}[\epsilon_1, \epsilon_2, \dots, \epsilon_M]$ (and it is invertible [55]), $\vec{\mathcal{U}} = (1, 1, \dots, 1)^\top$, an R -component vector, $\vec{\mathcal{N}} = (n_1^*, n_2^*, \dots, n_M^*)^\top$, $\vec{\mathcal{B}} = (\beta_1, \beta_2, \dots, \beta_M)^\top$, $\vec{\mathcal{L}} = (\Lambda_1, \Lambda_2, \dots, \Lambda_R)^\top$, and $\vec{\mathcal{X}} =$

$(c_1^*, c_2^*, \dots, c_R^*)^\top$. In Eq. (3) we have imposed the condition that all species, present at the initial time, have survived at a large-time, i.e., $(\vec{\mathcal{N}})_\sigma = n_\sigma^* > 0 \forall \sigma$. Later, we will also discuss and analyze the case when a sub-set of them go extinct.

Now, substituting Eq. (3) in Eq. (4), we find

$$GQ^T E^{-1} QG \vec{\mathcal{U}} - GQ^T E^{-1} \vec{\mathcal{B}} = \mu(\vec{\mathcal{L}} - \vec{\mathcal{X}}), \quad (5)$$

which gives R coupled equations that can be solved for $r_i(c_i^*)$ as a function of other parameters. Further, the condition for all species to survive can be written using Eq. (3):

$$(QG \vec{\mathcal{U}})_\sigma > \vec{\mathcal{B}}_\sigma \quad \forall \sigma, \quad (6)$$

and it gives the coexistence region in the R -dimensional space whose axes are $r_1(c_1^*), r_2(c_2^*), \dots, r_R(c_R^*)$. Thus, a necessary condition for all initial species to coexist is that the solution of Eq. (5) lies in the coexistence region; otherwise, some of them get extinct. This is our first main result.

To illuminate the above result, we first consider a case when several species are competing for one resource. A discussion for higher number of resources is relegated to the supplemental material [42]. In what follows, unless specified, we consider E to be a diagonal matrix [see Eq. (1)]. In this case, removing the immaterial index i , Eq. (3) becomes $n_\sigma^* = [\alpha_\sigma r(c^*) - \beta_\sigma] / \epsilon_\sigma$ for all σ . Since $n_\sigma^* > 0$, we find $r(c^*) > \beta_\sigma / \alpha_\sigma$. Moreover, we can write $r(c^*) > r(\bar{c}) \equiv \max_\sigma \{\beta_\sigma / \alpha_\sigma\}$, where $r(c^*)$ is the solution of Eq. (5): $Ar^2(c^*) - Br(c^*) - \mu(\Lambda - c^*) = 0$, in which the coefficients $A = \sum_\sigma \alpha_\sigma^2 / \epsilon_\sigma$ and $B = \sum_\sigma \alpha_\sigma \beta_\sigma / \epsilon_\sigma$ carry the characteristic features of the species. Note that $r(c^*) \leq 1$, therefore, the metabolic strategies, in order to guarantee a coexistence of all species, should be greater than the death rates: $\alpha_\sigma > \beta_\sigma$. Thus, for fixed parameters that characterize the species, i.e., $\{\alpha_\sigma, \beta_\sigma, \epsilon_\sigma\}$, coexistence of all species is achieved when tuning the resource supply rate by varying Λ at a fixed μ in such a way that the condition $r(c^*) > r(\bar{c})$ is satisfied. Such a critical value of Λ is given by $\bar{\Lambda} = r(\bar{c})[Ar(\bar{c}) - B] / \mu + \bar{c}$. In Fig. 1, we consider an example of ecosystem having 4 species competing for 1 resource. Clearly, when $\Lambda > \bar{\Lambda}$, all initial species survive (shown by solid lines), while some of them go extinct in the contrasting case.

In the following, we discuss how many species survive while competing for a single resource starting from some initial number of species M . For simplicity, in what follows, we consider $\beta_\sigma = 1$. Nevertheless, the analysis can also be done along the same line for generic β_σ 's. Since now each species is characterized by a set of parameters, one can define an array $\{\alpha_1, \epsilon_1; \alpha_2, \epsilon_2; \dots; \alpha_M, \epsilon_M\}$, where species are arranged according to decreasing metabolic strategies (see supplemental material for more details [42]). Further, we define two conditional sums: $A_l^{(c)} = \sum_{\sigma=1}^l \alpha_\sigma^2 / \epsilon_\sigma$, $B_l^{(c)} =$

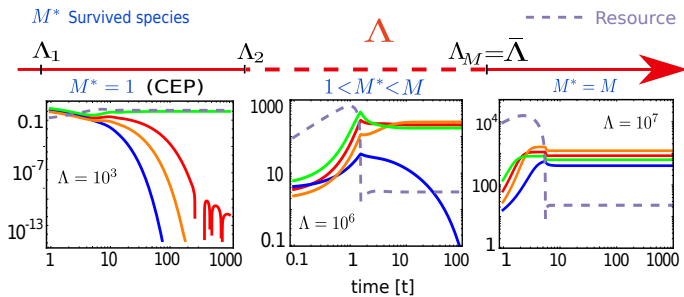


FIG. 1: Coexistence of species competing for 1 resource. Horizontal arrow indicates a schematic for Λ such that l number of species coexist if $\Lambda_l < \Lambda < \Lambda_{l+1}$ with $\Lambda_{M+1} = \infty$. We verify these results by numerically evolving the dynamics (1) and (2) for 4 species ($M = 4$, solid lines) competing for one resource ($R = 1$, dashed line). Clearly, for $\Lambda < \bar{\Lambda}$, the number of survived species M^* is less than M .

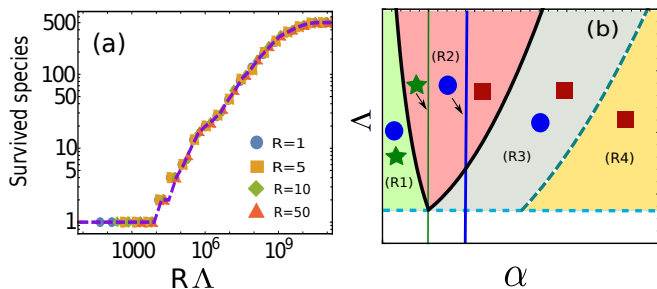


FIG. 2: Survival of species with Λ . (a) We compare the number of survived species obtained from numerical simulation (circles) of dynamics (1) and (2) for $R = 1$ with the theoretical prediction (dashed curve) (see text) for initial 500 species. Moreover, we compare the simulations results of $R = 1$ with $R > 1$ (square, diamond, and triangle). Clearly, all these curves collapse to each other when one rescales Λ with R (simulation details for $R > 1$ are relegated to Supplemental Material [42]). (b) Schematic of invasion by a third species (square) in a pool of two coexisting species (star and circle) competing for one resource. Two vertical lines correspond to metabolic strategies of two species (thicker for the fitter one, i.e., circle). We plot $\bar{\Lambda}$ (see main text), shown by a black solid curve [enclosing the region (R2)], that gives the critical resource supply for all of them to coexist as a function of metabolic strategy α of the invader for other fixed parameters. The dashed curve separating (R3) and (R4) corresponds to $\bar{\Lambda}$ for square and circle to coexist. The horizontal dashed line is the threshold Λ above which circle and star coexist in the absence of invader. Four different regions (R1)–(R4) are shown depending on the survival of species.

$\sum_{\sigma=1}^l \alpha_{\sigma} \beta_{\sigma} / \epsilon_{\sigma}$, where $1 \leq l \leq M$. Next, similar to the case when all species coexist, we find $\Lambda_l = \tilde{r}(\bar{c}) [A_l^{(c)} \tilde{r}(\bar{c}) - B_l^{(c)}] / \mu + k \tilde{r}(\bar{c}) / [1 - \tilde{r}(\bar{c})]$, the critical supply for l species in which $\tilde{r}(\bar{c}) = \max\{\alpha_{\sigma}^{-1} \mid 1 \leq \sigma \leq l\} \equiv \alpha_l^{-1}$. Thus, if $\Lambda_l < \Lambda < \Lambda_{l+1}$ then l species survive, $l = 1, 2, \dots, M$, where we have defined $\Lambda_{M+1} \equiv \infty$. In Fig. 1, we show both Λ_1 and Λ_2 (left markers) within which only the fittest species survives. We verify this result in Fig. 1

by numerically evolving the dynamics (1) and (2) for 4 species competing for one resource.

In Fig. 2(a), we compare the theoretical prediction using Λ_l for the number of coexisting species (dashed curve) with numerical simulations (circles) of Eqs. (1) and (2) for initial 500 species, and they have an excellent match. Moreover, we show the comparison for number of survived/coexisting species as R increases (see details in Supplemental Material [42]). Interestingly, we find that the simulation data for $R > 1$ collapse on the theoretical prediction for $R = 1$ when the resource supply is scaled with the number of resources. This is because for the same number of species to coexist a less resource supply for each resource is required, as expected.

Thus, by simply taking into account the spatial effects through intra-species competition, we conclude that a new phase emerges in addition to the phase where the number of coexisting species satisfies CEP. In the new phase, a finite fraction of all species coexists, regardless of the number of resources, and it saturates to 1 at a finite resource rate.

By exploiting the diagram [Fig. 2(a)], we now consider a pool of several coexisting species in the presence of one resource, and ask if a new species enters in the community, when it will successfully invade or coexist with the other species? To answer this question, for convenience, we consider a system of two coexisting species consuming one resource (Λ above the dashed line) and a third one arrives [see a circle, a star, and a square (invader) in the schematic shown in Fig. 2(b)]. Four different regimes [i.e., (R1)–(R4)] can be seen in Fig. 2(b) depending on the various possibilities of surviving species. These can be physically understood as follows. For a given Λ (above the dashed line), only star and circle could survive in region (R1) since Λ is lower than the black solid curve. In (R2), Λ is higher than the black curve, and therefore, we see coexistence. (R3) is the contrasting case to (R1), and finally, in (R4), the chosen Λ is lower than the dashed curve indicating that the invader can successfully invade the system (see supplemental material [42] for numerical simulation for each region).

In addition to the prediction of the critical value of Λ for the coexistence of a certain number of species and the related invasibility problem, our framework also allows us to determine the abundance distribution (SAD) of the surviving species, i.e., the probability $P(z)$ that a species has population size z . Interestingly, we can obtain the exact $P(z)$ for both one resource case and a large number of resources (the calculations of the latter are presented in the supplemental material [42]). Nonetheless, for intermediate number of resources, $P(z)$ can be easily computed numerically.

Let us first consider the case, when all initial species survive. Herein, we find $n_{\sigma}^* = [\alpha_{\sigma} r(c^*) - 1] / \epsilon_{\sigma} > 0$ [see Eq. (3)]. Now, we notice that for a large number of species, one can think of the parameters α_{σ} and ϵ_{σ}

to be random variables to incorporate the species variability and their differences. The stochasticity of these variables hinges on the way these are distributed among species. Let $Q_1(\alpha)$ and $Q_2(\epsilon)$, respectively, be the distributions for α and ϵ [56]. Three different scenarios can be investigated: (1) α distributed as a non-trivial Q_1 and $Q_2(\epsilon) = \delta(\epsilon - \hat{\epsilon})$, (2) $Q_1(\alpha) = \delta(\alpha - \hat{\alpha})$ and ϵ distributed as a non-trivial Q_2 , and (3) both are non-trivial stochastic variables. In the first scenario (1), the population distribution can be shown as [42] $P(z) = \hat{\epsilon} Q_1[(\hat{\epsilon}z + 1)/r(c^*)]/r(c^*)$, in the second scenario (2), we find [42] $P(z) = [\hat{\alpha}r(c^*) - 1]Q_2([\hat{\alpha}r(c^*) - 1]/z)/z^2$, and finally in (3), we find the distribution (see supplemental material for details [42]):

$$P(z) = \frac{[J_1(c, z) - J_1(d, z)]}{2z^2(q - p)(d - c)}, \quad (7)$$

where $J_1(\kappa, z) = [(q^2 - \kappa^2 z^2)\Theta(\kappa - p/z) + (q^2 - p^2)\Theta(p/z - \kappa)]\Theta(q/z - \kappa)$ in which $p = ar(c^*) - 1$ and $q = br(c^*) - 1$. The above expression (7) is obtained for uniformly distributed $\alpha \in \mathcal{U}(a, b)$ and $\epsilon \in \mathcal{U}(c, d)$. Nonetheless, for any other distributions, the population distribution $P(z)$ can also be computed [42]. This is our second main result.

In the case when the resource supply is limited, as we discussed above, some of the species will extinct at a large-time starting from some initial number of species. Herein, one can also compute the exact population distribution of the surviving species $P(z)$, and it is given by [42]:

$$P(z) = \frac{J_2(c, z) - J_2(d, z)}{2z^2q(d - c)}, \quad (8)$$

where $J_2(\kappa, z) = (q^2 - \kappa^2 z^2)\Theta(q/z - \kappa)$. However, the distribution of all species will be $P(z) = f_e \delta(z) + f_s P(z)$, where $f_s = 1 - f_e$ is the fraction of species survive and f_e is the extinction fraction. Once again, for simplicity, we have considered the case when $\alpha \in \mathcal{U}(a, b)$ and $\epsilon \in \mathcal{U}(c, d)$ are uniformly distributed.

In Fig. 3, we plot the complementary cumulative distribution function (CCDF) $F(z) = \int_z^\infty dy P(y)$ of population of the coexisting species for two scenarios: (a) when all of them coexist, and (b) when some of them go extinct. The exact predictions (dashed curves in Fig. 3) in panels (a) and (b), respectively, are shown for Eq. (7) and Eq. (8) for the case of a single resource. Finally, we emphasize that in most of the cases (including a large number of resources [42]), the distribution $P(z)$ has power-law tails with exponent -2 , i.e., $P(z) \sim z^{-2}$ as $z \rightarrow \infty$.

As mentioned above, one of the celebrated examples where several species coexist even in the presence of a few resources is the ocean plankton [12]. Recently, it has also been observed that species in plankton communities have a distribution of population sizes, as estimated by metagenomic studies, that decays as a steep power-law

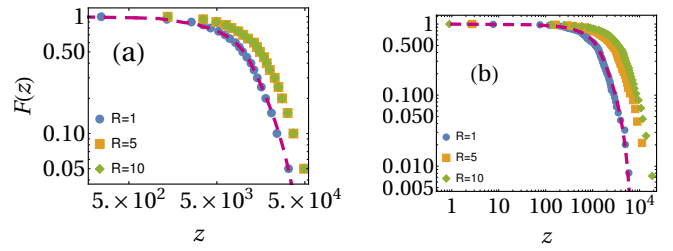


FIG. 3: Complementary cumulative distribution function (CCDF) for population of coexisting species. Panel (a): Species CCDF, $F(z)$, is shown when all species coexist. Panel (b): $F(z)$ is shown for surviving species starting from an initial number of species M . Circles are obtained by numerically integrating Eqs. (1) and (2) for large-time $t = 10^8$ for $M = 500$ and one resource while dashed line is the analytical prediction of CCDF: $F(z) = \int_z^\infty dy P(y)$, from Eq. (7) for panel (a) and Eq. (8) for panel (b). Squares and diamonds, respectively, are the numerical simulations when the number of resources is $R = 5$ and 10 . All cases exhibit a similar trend. The details of simulation for $R > 1$ and other fixed parameters are relegated to the supplemental material [42].

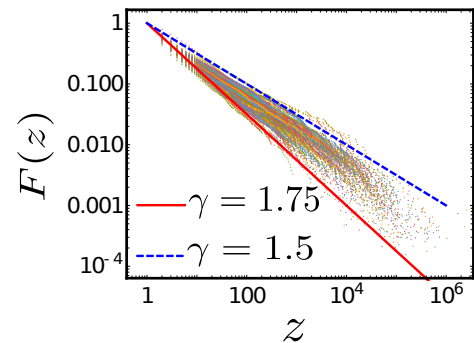


FIG. 4: Empirical CCDF for 134 surface seawater samples of microplankton obtained from the Tara ocean expedition [49, 50] (each color indicate one station). The lines are theoretical prediction of the power-law decay $F(z) \propto z^{-\gamma+1}$ with exponents between $\gamma_l = 1.5$ (blue dashed line) and $\gamma_u = 1.75$ (red solid line) (see text and [42]).

[50, 51]. Here we consider data on microplankton (20-180 μm in body size) from the Tara ocean expedition [49] (for more details, see [50], from which the data have been taken). In Fig. 4, we compare the empirical SADs (colored points) constructed from 134 surface seawater samples distributed over all the oceans [50], where each color corresponds to one station (thus 134 colors in total) with SAD obtained from stationary solution of our extended consumer-resource model (solid and dashed lines): $F(z) = \int_z^\infty P(x)dx \propto z^{-\gamma+1}$ for two “extreme” slopes $\gamma = \gamma_l = 1.5$ and $\gamma = \gamma_u = 1.75$ that we obtain from our model by considering a simple setting in which all species have the same α , whereas ϵ -s follow a power-law distribution: $Q_2(\epsilon) \sim \epsilon^{\gamma-2}$, for small ϵ , with $\gamma \in (1, 2]$

[see [42] for details and also the case in which the α -s are randomly distributed]. Finally, we stress that a range of exponents between γ_l and γ_u can be reproduced by appropriate tuning of parameter γ in $Q_2(\epsilon)$.

In summary, we have extended the consumer-resource model by incorporating the intra-species contributions that arise by coarse-graining the spatial degrees of freedom. This model could predict how several species coexist even for a relatively small number of resources. Further, we obtained analytically the distribution of the population sizes for one and a large number of resources. Our results are supported with the numerical simulations as well as the empirical prediction of SAD on the plankton discussed in Ref. [50].

Acknowledgements.— D.G., S.S., and A.M. are supported by “Excellence Project 2018” of the Cariparo foundation. S.S. acknowledges the Department of Physics and Astronomy from the University of Padova for funding through BIRD209912 project. S.G. acknowledges the support from Univeristy of Padova through the PhD fellowship within “Bando Dottorati di Ricerca” funded by the Cariparo foundation.

* These authors equally contributed to this work

- [1] A. Sher and M.C. Molles. Ecology: Concepts and Applications. McGraw-Hill Education, 2018.
- [2] John N Thompson. The coevolutionary process. University of Chicago press, 1994.
- [3] Dolph Schluter. The ecology of adaptive radiation. OUP Oxford, 2000.
- [4] Peter Chesson and Nancy Huntly. The roles of harsh and fluctuating conditions in the dynamics of ecological communities. The American Naturalist, 150(5):519–553, 1997.
- [5] Peter Chesson. Mechanisms of maintenance of species diversity. Annual review of Ecology and Systematics, 31(1):343–366, 2000.
- [6] TLS Vincent, D Scheel, JS Brown, and TL Vincent. Trade-offs and coexistence in consumer-resource models: it all depends on what and where you eat. The American Naturalist, 148(6):1038–1058, 1996.
- [7] Kenneth A Schmidt, Sasha RX Dall, and Jan A Van Gils. The ecology of information: an overview on the ecological significance of making informed decisions. Oikos, 119(2):304–316, 2010.
- [8] Jonathan M Chase and Mathew A Leibold. Ecological niches: linking classical and contemporary approaches. University of Chicago Press, 2003.
- [9] Francesco Carrara, Andrea Giometto, Mathew Seymour, Andrea Rinaldo, and Florian Altermatt. Inferring species interactions in ecological communities: a comparison of methods at different levels of complexity. Methods in Ecology and Evolution, 6(8):895–906, 2015.
- [10] Aleksej Zelezniak, Sergej Andrejev, Olga Ponomarova, Daniel R. Mende, Peer Bork, and Kiran Raosaheb Patil. Metabolic dependencies drive species co-occurrence in diverse microbial communities. Proceedings of the National Academy of Sciences, 112(20):6449–6454, 2015.
- [11] Joshua E. Goldford, Nanxi Lu, Djordje Bajić, Sylvie Estrela, Mikhail Tikhonov, Alicia Sanchez-Gorostiaga, Daniel Segrè, Pankaj Mehta, and Alvaro Sanchez. Emergent simplicity in microbial community assembly. Science, 361(6401):469–474, 2018.
- [12] G. E. Hutchinson. The paradox of the plankton. The American Naturalist, 95(882):137–145, 1961.
- [13] Robert Mac Arthur. Species packing, and what competition minimizes. Proceedings of the National Academy of Sciences, 64(4):1369–1371, 1969.
- [14] Peter Chesson. Macarthur’s consumer-resource model. Theoretical Population Biology, 37(1):26 – 38, 1990.
- [15] Garrett Hardin. The competitive exclusion principle. Science, 131(3409):1292–1297, 1960.
- [16] Robert MacArthur and Richard Levins. Competition, habitat selection, and character displacement in a patchy environment. Proceedings of the National Academy of Sciences, 51(6):1207–1210, 1964.
- [17] Simon A. Levin. Community equilibria and stability, and an extension of the competitive exclusion principle. The American Naturalist, 104(939):413–423, 1970.
- [18] Richard McGehee and Robert A Armstrong. Some mathematical problems concerning the ecological principle of competitive exclusion. Journal of Differential Equations, 23(1):30–52, 1977.
- [19] Robert A Armstrong and Richard McGehee. Competitive exclusion. The American Naturalist, 115(2):151–170, 1980.
- [20] NF Britton. Aggregation and the competitive exclusion principle. Journal of Theoretical Biology, 136(1):57–66, 1989.
- [21] Alexandru Hening and Dang H Nguyen. The competitive exclusion principle in stochastic environments. Journal of mathematical biology, 80(5):1323–1351, 2020.
- [22] Anna Posfai, Thibaud Tallefumier, and Ned S. Wingreen. Metabolic trade-offs promote diversity in a model ecosystem. Phys. Rev. Lett., 118:028103, Jan 2017.
- [23] Leonardo Pacciani-Mori, Andrea Giometto, Samir Suweis, and Amos Maritan. Dynamic metabolic adaptation can promote species coexistence in competitive microbial communities. PLOS Computational Biology, 16(5):1–18, 05 2020.
- [24] Leonardo Pacciani-Mori, Samir Suweis, Amos Maritan, and Andrea Giometto. Constrained proteome allocation affects coexistence in models of competitive microbial communities. bioRxiv, 2020.
- [25] Shovonlal Roy and J. Chattopadhyay. The stability of ecosystems: A brief overview of the paradox of enrichment. Journal of Biosciences, 32:421 – 428, 2007.
- [26] Akshit Goyal, Veronika Dubinkina, and Sergei Maslov. Multiple stable states in microbial communities explained by the stable marriage problem. The ISME Journal, 12:2823–2834, 12 2018.
- [27] Hal Caswell. Community structure: a neutral model analysis. Ecological monographs, 46(3):327–354, 1976.
- [28] Stephen P Hubbell. Tree dispersion, abundance, and diversity in a tropical dry forest. Science, 203(4387):1299–1309, 1979.
- [29] Stephen P Hubbell. The unified neutral theory of biodiversity and biogeography (MPB-32), volume 32. Princeton University Press, 2001.

- [30] M Vallade, , and B Houchmandzadeh. Analytical solution of a neutral model of biodiversity. *Physical Review E*, 68(6):061902, 2003.
- [31] Jérôme Chave. Neutral theory and community ecology. *Ecology letters*, 7(3):241–253, 2004.
- [32] David Alonso, Rampal S Etienne, and Alan J McKane. The merits of neutral theory. *Trends in ecology & evolution*, 21(8):451–457, 2006.
- [33] James Rosindell, Stephen P Hubbell, and Rampal S Etienne. The unified neutral theory of biodiversity and biogeography at age ten. *Trends in ecology & evolution*, 26(7):340–348, 2011.
- [34] Sandro Azaele, Samir Suweis, Jacopo Grilli, Igor Volkov, Jayanth R Banavar, and Amos Maritan. Statistical mechanics of ecological systems: Neutral theory and beyond. *Reviews of Modern Physics*, 88(3):035003, 2016.
- [35] Stephen P Hubbell. A unified theory of biogeography and relative species abundance and its application to tropical rain forests and coral reefs. *Coral reefs*, 16(1):S9–S21, 1997.
- [36] Igor Volkov, Jayanth R Banavar, Stephen P Hubbell, and Amos Maritan. Neutral theory and relative species abundance in ecology. *Nature*, 424(6952):1035–1037, 2003.
- [37] Sandro Azaele, Simone Pigolotti, Jayanth R Banavar, and Amos Maritan. Dynamical evolution of ecosystems. *Nature*, 444(7121):926–928, 2006.
- [38] Fabio Peruzzo, Mauro Mobilia, and Sandro Azaele. Spatial patterns emerging from a stochastic process near criticality. *Physical Review X*, 10(1):011032, 2020.
- [39] Graham Bell. The distribution of abundance in neutral communities. *The American Naturalist*, 155(5):606–617, 2000.
- [40] Graham Bell. Neutral macroecology. *Science*, 293(5539):2413–2418, 2001.
- [41] Enrico Ser-Giacomi, Lucie Zinger, Shruti Malviya, Colomban De Vargas, Eric Karsenti, Chris Bowler, and Silvia De Monte. Ubiquitous abundance distribution of non-dominant plankton across the global ocean. *Nature Ecology & Evolution*, 2:1243–1249, 08 2018.
- [42] Gupta Deepak, Garlaschi Stefano, Suweis Samir, Azaele Sandro, and Maritan Amos. Supplemental matrial.
- [43] Daniel H Janzen. Herbivores and the number of tree species in tropical forests. *The American Naturalist*, 104(940):501–528, 1970.
- [44] Joseph H Connell. On the role of natural enemies in preventing competitive exclusion in some marine animals and in rain forest trees. *Dynamics of populations*, 298:312, 1971.
- [45] Eugene W. Schupp. The janzen-connell model for tropical tree diversity: Population implications and the importance of spatial scale. *The American Naturalist*, 140(3):526–530, 1992.
- [46] Deborah A Clark and David B Clark. Spacing dynamics of a tropical rain forest tree: evaluation of the janzen-connell model. *The American Naturalist*, 124(6):769–788, 1984.
- [47] Robert Bagchi, Tom Swinfield, Rachel E Gallery, Owen T Lewis, Sofia Gripenberg, Lakshmi Narayan, and Robert P Freckleton. Testing the janzen-connell mechanism: pathogens cause overcompensating density dependence in a tropical tree. *Ecology letters*, 13(10):1262–1269, 2010.
- [48] Robert Bagchi, Rachel E Gallery, Sofia Gripenberg, Sarah J Gurr, Lakshmi Narayan, Claire E Addis, Robert P Freckleton, and Owen T Lewis. Pathogens and insect herbivores drive rainforest plant diversity and composition. *Nature*, 506(7486):85–88, 2014.
- [49] Colomban De Vargas, Stéphane Audic, Nicolas Henry, Johan Decelle, Frédéric Mahé, Ramiro Logares, Enrique Lara, Cédric Berney, Noan Le Bescot, Ian Probert, et al. Eukaryotic plankton diversity in the sunlit ocean. *Science*, 348(6237), 2015.
- [50] Enrico Ser-Giacomi, Lucie Zinger, Shruti Malviya, Colomban De Vargas, Eric Karsenti, Chris Bowler, and Silvia De Monte. Ubiquitous abundance distribution of non-dominant plankton across the global ocean. *Nature ecology & evolution*, 2(8):1243–1249, 2018.
- [51] Paula Villa Martin, Ales Bucek, Tom Bourguignon, and Simone Pigolotti. Ocean currents promote rare species diversity in protists. *bioRxiv*, 2020.
- [52] Evelyn F. Keller and Lee A. Segel. Model for chemotaxis. *Journal of Theoretical Biology*, 30(2):225–234, 1971.
- [53] Kenneth G. Wilson. The renormalization group: Critical phenomena and the kondo problem. *Rev. Mod. Phys.*, 47:773–840, Oct 1975.
- [54] Shang-keng Ma and Gene F. Mazenko. Critical dynamics of ferromagnets in $6 - \epsilon$ dimensions: General discussion and detailed calculation. *Phys. Rev. B*, 11:4077–4100, Jun 1975.
- [55] The representation of Eq. (3) could also be useful even in the case when matrix E is not diagonal, for e.g., in the case when the last term in the parenthesis in Eq. (1) is replaced by $\sum_{\gamma} \epsilon_{\sigma\gamma} n_{\gamma}$.
- [56] Note that we have dropped the subscript σ for convenience.
-

Supplemental Material for “An Effective Resource-Competition Model for Species Coexistence”

EMERGENCE OF THE NEW CARRYING CAPACITY TERM

In this section, we present an argument that justifies how the carrying capacity like term, emerges quite generally in the consumer-resource model although it has a clear ecological interpretation by itself. In order to do so, we apply a coarse graining procedure on a spatially extended consumer-resource model where we integrate out some degrees of freedom, and then, obtain an effective mean-field dynamics for the remaining ones.

Let us start by considering the MacArthur’s model for one species consuming only one resource. Thus there is no need for sub-indices for species and resources. To include spatial contributions in the dynamics, we add flux-terms motivated by the seminal work of Keller and Segel [52] in which the flux of the motion of species in the environment of resources are expressed as

$$J_n(x, t) = -D_1(c(x, t)) \nabla n(x, t) + D_2(c(x, t)) n(x, t) \nabla c(x, t), \quad (\text{S1})$$

which can be written as (in the leading order in c) as

$$J_n(x, t) = -(A_1 + \delta A_2 c(x, t)) \nabla n(x, t) + \delta A_3 n(x, t) \nabla c(x, t). \quad (\text{S2})$$

where A_1 , A_2 , and A_3 are constants. δ is a constant introduced for future purposes in front of the coefficients of the terms quadratic in the dynamical variables of the system.

Therefore, the systems’ dynamics is given by

$$\dot{n}(x, t) = n(x, t)(\delta \alpha c(x, t) - \beta) - \nabla J_n(x, t), \quad (\text{S3})$$

$$\dot{c}(x, t) = s - \mu c(x, t) - \delta \alpha n(x, t) c(x, t), \quad (\text{S4})$$

where we wrote the α terms with an δ contribution since they are quadratic in $n(x, t)$ and $c(x, t)$. Notice that we replaced the Monod function with $c(x, t)$, which is the leading order in a small c expansion.

Substituting J_n from Eq. (S2), we rewrite Eqs (S3) and (S4) as

$$\begin{aligned} \dot{n}(x, t) &= n(x, t)(\delta \alpha c(x, t) - \beta) + (A_1 + \delta A_2 c(x, t)) \nabla^2 n(x, t) \\ &\quad - \delta A_3 n(x, t) \nabla^2 c(x, t) + \delta(A_2 - A_3) \nabla n(x, t) \cdot \nabla c(x, t), \end{aligned} \quad (\text{S5})$$

$$\dot{c}(x, t) = s - \mu c(x, t) - \delta \alpha n(x, t) c(x, t). \quad (\text{S6})$$

Next we consider the case in which the spatial variable is discrete in a one-dimensional lattice, where each site, i , represents a patch of linear size a with a population n_i and a resource concentration c_i . Notice that now the sub-indices refer to spatial position and not to species or resource. Therefore, we have

$$\begin{aligned} \dot{n}_i(t) &= n_i(t)[\delta \alpha c_i(t) - \beta] + [A_1 + \delta A_2 c_i(t)] [n_{i+i}(t) + n_{i-i}(t) - 2n_i(t)] + \\ &\quad - \delta A_3 n_i(t) [c_{i+i}(t) + c_{i-i}(t) - 2c_i(t)] + \delta(A_2 - A_3) [n_{i+i}(t) - n_i(t)] [c_{i+i}(t) - c_i(t)], \end{aligned} \quad (\text{S7})$$

$$\dot{c}_i(t) = s - \mu c_i(t) - \delta \alpha n_i(t) c_i(t), \quad (\text{S8})$$

where $i \in \mathbb{Z}$ indicates the lattice site or the label for the patch. Thus, this model [Eqs. (S7) and (S8)] describes the migration of species from one patch to another for the consumption of the resource.

The coarse-graining consists in eliminating the dynamical variables c_i and n_i corresponding to the odd positions in favour of the remaining ones in the even positions in the same spirit as in the first step of the renormalization group technique (see Refs. [53, 54]). The essence of the calculation can be exemplified by considering just two adjacent sites/patches $i = 1, 2$ and periodic boundary conditions. The complete calculation, besides being more cumbersome, does not present any technical difficulty and leads to the same result of inducing the carrying capacity term, n_σ^2 , in Eq.(1) of the main text. Hence, the dynamics given in Eqs. (S7) and (S8) can be rewritten as

$$\dot{n}_1 = n_1(\delta \alpha c_1 - \beta) + 2A_1(n_2 - n_1) + \delta(A_2 - A_3)(n_2 c_2 - n_1 c_1) + \delta(A_2 + A_3)(n_2 c_1 - n_1 c_2), \quad (\text{S9})$$

$$\dot{n}_2 = n_2(\delta \alpha c_2 - \beta) + 2A_1(n_1 - n_2) + \delta(A_2 - A_3)(n_1 c_1 - n_2 c_2) + \delta(A_2 + A_3)(n_1 c_2 - n_2 c_1), \quad (\text{S10})$$

$$\dot{c}_1 = s - \mu c_1 - \delta \alpha n_1 c_1, \quad (\text{S11})$$

$$\dot{c}_2 = s - \mu c_2 - \delta \alpha n_2 c_2, \quad (\text{S12})$$

where for convenience we are not writing explicitly the time dependence.

In order to proceed forward, let us first define Laplace transform and its inverse as follow

$$\tilde{\Omega}(\omega) = \mathcal{L}[\Omega(t)](\omega) = \int_0^{+\infty} dt e^{-\omega t} \Omega(t), \quad (\text{S13})$$

$$\Omega(t) = \mathcal{L}^{-1}[\tilde{\Omega}(\omega)](t) = \frac{1}{2\pi i} \lim_{\gamma \rightarrow \infty} \int_{a-i\gamma}^{a+i\gamma} d\omega e^{\omega t} \tilde{\Omega}(\omega), \quad (\text{S14})$$

where a is such that all singularities of $\tilde{\Omega}(\omega)$ are in the region $\Re(\omega) < a$.

Now Laplace transform [defined in Eq. (S13)] of Eqs. (S9)–(S12) gives

$$\omega \tilde{n}_1(\omega) - n_1(0) = -\beta \tilde{n}_1(\omega) + \delta \alpha \tilde{n}_1(\omega) * \tilde{c}_1(\omega) + 2A_1(\tilde{n}_2(\omega) - \tilde{n}_1(\omega)) + \delta(A_2 - A_3)(\tilde{n}_2(\omega) * \tilde{c}_2(\omega) - \tilde{n}_1(\omega) * \tilde{c}_1(\omega)) + \delta(A_2 + A_3)(\tilde{n}_2(\omega) * \tilde{c}_1(\omega) - \tilde{n}_1(\omega) * \tilde{c}_2(\omega)), \quad (\text{S15})$$

$$\omega \tilde{n}_2(\omega) - n_2(0) = -\beta \tilde{n}_2(\omega) + \delta \alpha \tilde{n}_2(\omega) * \tilde{c}_2(\omega) + 2A_1(\tilde{n}_1(\omega) - \tilde{n}_2(\omega)) + \delta(A_2 - A_3)(\tilde{n}_1(\omega) * \tilde{c}_1(\omega) - \tilde{n}_2(\omega) * \tilde{c}_2(\omega)) + \delta(A_2 + A_3)(\tilde{n}_1(\omega) * \tilde{c}_2(\omega) - \tilde{n}_2(\omega) * \tilde{c}_1(\omega)), \quad (\text{S16})$$

$$\omega \tilde{c}_1(\omega) - c_1(0) = \tilde{s}(\omega) - \mu \tilde{c}_1(\omega) - \delta \alpha \tilde{n}_1(\omega) * \tilde{c}_1(\omega), \quad (\text{S17})$$

$$\omega \tilde{c}_2(\omega) - c_2(0) = \tilde{s}(\omega) - \mu \tilde{c}_2(\omega) - \delta \alpha \tilde{n}_2(\omega) * \tilde{c}_2(\omega), \quad (\text{S18})$$

where $n_i(0)$ and $c_i(0)$ are the initial conditions of the system and the symbol $*$ indicates the convolution of the functions in the complex plane defined as

$$\mathcal{L}[n_2(t)c_1(t)](\omega) = \tilde{n}_2(\omega) * \tilde{c}_1(\omega) = \frac{1}{2\pi i} \lim_{\gamma \rightarrow \infty} \int_{a-i\gamma}^{a+i\gamma} d\sigma \tilde{n}_2(\sigma) c_1(\omega - \sigma) \quad (\text{S19})$$

We can recast Eqs. (S15)–(S18) as follows:

$$(\omega + \beta + 2A_1) \tilde{n}_1(\omega) = n_1(0) + 2A_1 \tilde{n}_2(\omega) + \delta \left\{ \alpha \tilde{n}_1(\omega) * \tilde{c}_1(\omega) + (A_2 - A_3)(\tilde{n}_2(\omega) * \tilde{c}_2(\omega) - \tilde{n}_1(\omega) * \tilde{c}_1(\omega)) + (A_2 + A_3)(\tilde{n}_2(\omega) * \tilde{c}_1(\omega) - \tilde{n}_1(\omega) * \tilde{c}_2(\omega)) \right\}, \quad (\text{S20})$$

$$(\omega + \beta + 2A_1) \tilde{n}_2(\omega) = n_2(0) + 2A_1 \tilde{n}_1(\omega) + \delta \left\{ \alpha \tilde{n}_2(\omega) * \tilde{c}_2(\omega) + (A_2 - A_3)(\tilde{n}_1(\omega) * \tilde{c}_1(\omega) - \tilde{n}_2(\omega) * \tilde{c}_2(\omega)) + (A_2 + A_3)(\tilde{n}_1(\omega) * \tilde{c}_2(\omega) - \tilde{n}_2(\omega) * \tilde{c}_1(\omega)) \right\}, \quad (\text{S21})$$

$$(\omega + \mu) \tilde{c}_1(\omega) = c_1(0) + \tilde{s}(\omega) - \delta \alpha \tilde{n}_1(\omega) * \tilde{c}_1(\omega), \quad (\text{S22})$$

$$(\omega + \mu) \tilde{c}_2(\omega) = c_2(0) + \tilde{s}(\omega) - \delta \alpha \tilde{n}_2(\omega) * \tilde{c}_2(\omega). \quad (\text{S23})$$

We now employ a standard perturbative approach, where the expansion parameter is given by δ , in order to express $\tilde{n}_1(\omega)$ and $\tilde{c}_1(\omega)$ in terms of $\tilde{n}_2(\omega)$ and $\tilde{c}_2(\omega)$ up to terms of order δ^2 . Additionally we assume $n_1(0) = c_1(0) = 0$. Once this procedure has been carried out (the calculations are straightforward and yet cumbersome, so in order not to distract the reader we avoid the full presentation of all the intermediate steps), we can plug such expressions into Eq. (S21). In this way we remove from the dynamics the patch 1 by taking into account its contribution in an effective way. Neglecting order δ^3 terms or higher, we obtain

$$\begin{aligned} \omega \tilde{n}_2(\omega) - n_2(0) = & - \left(\beta + 2A_1 - \frac{4A_1^2}{\omega + \beta + 2A_1} \right) \tilde{n}_2(\omega) + \delta \left\{ \left(\alpha - A_2 + A_3 + \frac{2A_1(A_2 + A_3)}{\omega + \beta + 2A_1} \right) \tilde{n}_2(\omega) * \tilde{c}_2(\omega) + \right. \\ & + \frac{2A_1(A_2 + A_3)}{\omega + \beta + 2A_1} \left(\frac{\tilde{s}(\omega)}{\omega + \mu} \right) * \tilde{n}_2(\omega) + \frac{4A_1^2(\alpha - A_2 + A_3)}{\omega + \beta + 2A_1} \left(\frac{\tilde{n}_2(\omega)}{\omega + \beta + 2A_1} \right) * \left(\frac{\tilde{s}(\omega)}{\omega + \mu} \right) + \\ & - \frac{4A_1^2(A_2 + A_3)}{\omega + \beta + 2A_1} \left(\frac{\tilde{n}_2(\omega)}{\omega + \beta + 2A_1} \right) * \tilde{c}_2(\omega) + 2A_1(A_2 + A_3) \tilde{c}_2(\omega) * \left(\frac{\tilde{n}_2(\omega)}{\omega + \beta + 2A_1} \right) + \\ & \left. - (A_2 + A_3) \tilde{n}_2(\omega) * \left(\frac{\tilde{s}(\omega)}{\omega + \mu} \right) + 2A_1(A_2 - A_3) \left(\frac{\tilde{s}(\omega)}{\omega + \mu} \right) * \left(\frac{\tilde{n}_2(\omega)}{\omega + \beta + 2A_1} \right) \right\} + \\ & + \delta^2 \left\{ \frac{8A_1^3 \alpha (\alpha - A_2 + A_3)}{\omega + \beta + 2A_1} \left[\left(\frac{\tilde{n}_2(\omega)}{\omega + \beta + 2A_1} \right) * \left(\frac{\left(\frac{\tilde{n}_2(\omega)}{\omega + \beta + 2A_1} \right) * \left(\frac{\tilde{s}(\omega)}{\omega + \mu} \right)}{\omega + \mu} \right) \right] + \right. \\ & \left. - \frac{2A_1(A_2 - A_3)(A_2 + A_3)}{\omega + \beta + 2A_1} \left[\left(\frac{\tilde{n}_2(\omega) * \tilde{c}_2(\omega)}{\omega + \beta + 2A_1} \right) * \tilde{c}_2(\omega) \right] + \right. \end{aligned}$$

$$\begin{aligned}
& - \frac{4A_1^2\alpha(A_2 + A_3)}{\omega + \beta + 2A_1} \left[\left(\frac{\left(\frac{\tilde{s}(\omega)}{\omega + \mu} \right) * \left(\frac{\tilde{n}_2(\omega)}{\omega + \beta + 2A_1} \right)}{\omega + \mu} \right) * \tilde{n}_2(\omega) \right] + \\
& + \frac{4A_1^2(\alpha - A_2 + A_3)^2}{\omega + \beta + 2A_1} \left[\left(\frac{\tilde{s}(\omega)}{\omega + \mu} \right) * \left(\frac{\left(\frac{\tilde{s}(\omega)}{\omega + \mu} \right) * \left(\frac{\tilde{n}_2(\omega)}{\omega + \beta + 2A_1} \right)}{\omega + \beta + 2A_1} \right) \right] + \\
& + \frac{2A_1(A_2 - A_3)(\alpha - A_2 + A_3)}{\omega + \beta + 2A_1} \left[\left(\frac{\tilde{s}(\omega)}{\omega + \mu} \right) * \left(\frac{\tilde{n}_2(\omega) * \tilde{c}_2(\omega)}{\omega + \beta + 2A_1} \right) \right] + \\
& + \frac{2A_1(A_2 + A_3)(\alpha - A_2 + A_3)}{\omega + \beta + 2A_1} \left[\left(\frac{\tilde{s}(\omega)}{\omega + \mu} \right) * \left(\frac{\tilde{n}_2(\omega) * \left(\frac{\tilde{s}(\omega)}{\omega + \mu} \right)}{\omega + \beta + 2A_1} \right) \right] + \\
& - \frac{4A_1^2(A_2 + A_3)(\alpha - A_2 + A_3)}{\omega + \beta + 2A_1} \left[\left(\frac{\tilde{s}(\omega)}{\omega + \mu} \right) * \left(\frac{\tilde{c}_2(\omega) * \left(\frac{\tilde{n}_2(\omega) * \tilde{c}_2(\omega)}{\omega + \beta + 2A_1} \right)}{\omega + \beta + 2A_1} \right) \right] + \\
& - \frac{4A_1^2(A_2 + A_3)(\alpha - A_2 + A_3)}{\omega + \beta + 2A_1} \left[\tilde{c}_2(\omega) * \left(\frac{\left(\frac{\tilde{s}(\omega)}{\omega + \mu} \right) * \left(\frac{\tilde{n}_2(\omega) * \tilde{c}_2(\omega)}{\omega + \beta + 2A_1} \right)}{\omega + \beta + 2A_1} \right) \right] + \\
& - \frac{2A_1(A_2 + A_3)^2}{\omega + \beta + 2A_1} \left[\tilde{c}_2(\omega) * \left(\frac{\tilde{n}_2(\omega) * \left(\frac{\tilde{s}(\omega)}{\omega + \mu} \right)}{\omega + \beta + 2A_1} \right) \right] + \frac{4A_1^2(A_2 + A_3)^2}{\omega + \beta + 2A_1} \left[\tilde{c}_2(\omega) * \left(\frac{\tilde{c}_2(\omega) * \left(\frac{\tilde{n}_2(\omega)}{\omega + \beta + 2A_1} \right)}{\omega + \beta + 2A_1} \right) \right] + \\
& + 2A_1\alpha(A_2 + A_3) \left[\tilde{n}_2(\omega) * \left(\frac{\left(\frac{\tilde{s}(\omega)}{\omega + \mu} \right) * \left(\frac{\tilde{n}_2(\omega)}{\omega + \beta + 2A_1} \right)}{\omega + \mu} \right) \right] + \\
& + 2A_1(A_2 + A_3)(\alpha - A_2 + A_3) \left[\tilde{c}_2(\omega) * \left(\frac{\left(\frac{\tilde{s}(\omega)}{\omega + \mu} \right) * \left(\frac{\tilde{n}_2(\omega)}{\omega + \beta + 2A_1} \right)}{\omega + \mu} \right) \right] + \\
& + (A_2 + A_3)(A_2 - A_3) \left[\tilde{c}_2(\omega) * \left(\frac{\tilde{n}_2(\omega) * \tilde{c}_2(\omega)}{\omega + \beta + 2A_1} \right) \right] + (A_2 + A_3)^2 \left[\tilde{c}_2(\omega) * \left(\frac{\tilde{n}_2(\omega) * \left(\frac{\tilde{s}(\omega)}{\omega + \mu} \right)}{\omega + \beta + 2A_1} \right) \right] + \\
& - 2A_1(A_2 + A_3)^2 \left[\tilde{c}_2(\omega) * \left(\frac{\tilde{c}_2(\omega) * \left(\frac{\tilde{n}_2(\omega)}{\omega + \beta + 2A_1} \right)}{\omega + \beta + 2A_1} \right) \right] + \\
& - 4A_1^2\alpha(A_2 - A_3) \left[\left(\frac{\tilde{n}_2(\omega)}{\omega + \beta + 2A_1} \right) * \left(\frac{\left(\frac{\tilde{s}(\omega)}{\omega + \mu} \right) * \left(\frac{\tilde{n}_2(\omega)}{\omega + \beta + 2A_1} \right)}{\omega + \mu} \right) \right] + \\
& + 2A_1(A_2 - A_3)(\alpha - A_2 + A_3) \left[\left(\frac{\tilde{s}(\omega)}{\omega + \mu} \right) * \left(\frac{\left(\frac{\tilde{s}(\omega)}{\omega + \mu} \right) * \left(\frac{\tilde{n}_2(\omega)}{\omega + \beta + 2A_1} \right)}{\omega + \mu} \right) \right] + \\
& + (A_2 - A_3)^2 \left[\left(\frac{\tilde{s}(\omega)}{\omega + \mu} \right) * \left(\frac{\tilde{n}_2(\omega) * \tilde{c}_2(\omega)}{\omega + \beta + 2A_1} \right) \right] + (A_2 - A_3)(A_2 + A_3) \left[\left(\frac{\tilde{s}(\omega)}{\omega + \mu} \right) * \left(\frac{\tilde{n}_2(\omega) * \left(\frac{\tilde{s}(\omega)}{\omega + \mu} \right)}{\omega + \beta + 2A_1} \right) \right] + \\
& - 2A_1(A_2 - A_3)(A_2 + A_3) \left[\left(\frac{\tilde{s}(\omega)}{\omega + \mu} \right) * \left(\frac{\tilde{c}_2(\omega) * \left(\frac{\tilde{n}_2(\omega)}{\omega + \beta + 2A_1} \right)}{\omega + \beta + 2A_1} \right) \right] \} + \mathcal{O}(\delta^3) \tag{S24}
\end{aligned}$$

Since we are interested in the large-time limit, where both \tilde{n}_2 and \tilde{c}_2 are small, the above formula can be simplified

as follows. For example, the inverse Laplace transform of $\tilde{n}_2(\omega)/(\omega + \omega_0)$, with $\beta + 2A_1 \equiv \omega_0 > 0$, is:

$$\mathcal{L}^{-1} \left[\frac{\tilde{n}_2(\omega)}{\omega + \omega_0} \right] (t) = \int_0^t dt' n_2(t') e^{-\omega_0(t-t')} \quad (\text{S25})$$

$$= \frac{1}{\omega_0} \left(n_2(t) - n_2(0) e^{-t\omega_0} - \int_0^t dt' \dot{n}_2(t') e^{-\omega_0(t-t')} \right) \quad (\text{S26})$$

$$\approx \frac{n_2(t)}{\omega_0} \quad (\text{S27})$$

when $t \gg \omega_0^{-1}$. Notice that we use integration by parts to reach Eq. (S26) from Eq. (S25). In order to make this more formal we simply introduce a parameter τ multiplying the time derivatives in Eqs. (S9)–(S12). This leads to a simple modification of the Eq. (S24) where all ω 's are multiplied by τ except for the ω 's appearing as arguments of the functions $\tilde{n}_2(\omega)$, $\tilde{c}_2(\omega)$ and $\tilde{s}(\omega)$. In the small τ limit, and redefining $\tilde{n}_2(\omega)$ as

$$\tilde{n}'_2(\omega) \equiv \left[1 + \left(\frac{2A_1}{\beta + 2A_1} \right)^2 \right] \tilde{n}_2(\omega), \quad (\text{S28})$$

we get (now we drop the sub-indices)

$$\tau \dot{n}'(t) = n'(t) (\alpha' [c(t)] c(t) - \beta') - \epsilon' n'^2(t), \quad (\text{S29})$$

with

$$\begin{aligned} \beta' &= (C_1 + \delta s C_2 + \delta^2 s^2 C_3) \left[1 + \left(\frac{2A_1}{\beta + 2A_1} \right)^2 \right]^{-1} + \mathcal{O}(\tau\delta), \\ \alpha' [c_2(t)] &= (\delta C_4 + \delta^2 s C_5 + \delta^2 C_6 c_2(t)) \left[1 + \left(\frac{2A_1}{\beta + 2A_1} \right)^2 \right]^{-1} + \mathcal{O}(\tau\delta), \\ \epsilon' &= \delta^2 C_7 \left[1 + \left(\frac{2A_1}{\beta + 2A_1} \right)^2 \right]^{-2} + \mathcal{O}(\tau\delta^2), \end{aligned} \quad (\text{S30})$$

where

$$\begin{aligned} C_1 &= -\beta \left(\frac{\beta + 4A_1}{\beta + 2A_1} \right), \\ C_2 &= \left(\frac{4A_1 A_2}{\mu(\beta + 2A_1)} + \frac{4A_1^2(\alpha - A_2 + A_3)}{\mu(\beta + 2A_1)^2} - \frac{A_2 + A_3}{\mu} \right), \\ C_3 &= \left(\frac{4A_1^2(\alpha - A_2 + A_3)^2}{\mu^2(\beta + 2A_1)^3} + \frac{4A_1 A_2(\alpha - A_2 + A_3)}{\mu^2(\beta + 2A_1)^2} + \frac{A_2^2 - A_3^2}{\mu^2(\beta + 2A_1)} \right) \\ C_4 &= \left(\alpha - A_2 + A_3 + \frac{4A_1 A_2}{\beta + 2A_1} - \frac{4A_1^2(A_2 + A_3)}{(\beta + 2A_1)^2} \right), \\ C_5 &= \left(-\frac{8A_1^2(\alpha - A_2 + A_3)(A_2 + A_3)}{\mu(\beta + 2A_1)^3} + \frac{2(A_2^2 + A_3)^2}{\mu(\beta + 2A_1)} + \frac{4A_1 A_2(\alpha - 2A_2)}{\mu(\beta + 2A_1)^2} \right) \\ C_6 &= \left(-\frac{4A_1 A_2(A_2 + A_3)}{(\beta + 2A_1)^2} + \frac{4A_1^2(A_2 + A_3)^2}{(\beta + 2A_1)^3} + \frac{A_2^2 - A_3^2}{\beta + 2A_1} \right) \\ C_7 &= \left(\frac{8A_1^3(\alpha - A_2 + A_3)}{\mu^2(\beta + 2A_1)^3} + \frac{8A_1^2 A_2 \alpha}{\mu^2(\beta + 2A_1)^2} \right). \end{aligned} \quad (\text{S31})$$

Notice that the effect of the coarse-graining leads to a "renormalization" of the growth, the term linear in n , which is an expansion in the resource concentration, c , and in the resource supply, s . Finally the contribution ϵ' is the term we aimed to get for our model shown in Eqs. (1) and (2) in the main text. Therefore, as an effect of the coarse-graining, a carrying capacity term emerges in the effective evolution equations we dealt in the main text.

COEXISTENCE OF SPECIES IN THE PRESENCE OF TWO RESOURCES

In this section, we present the calculations to obtain the condition that ensures the coexistence of all initial species competing for two abiotic resources ($R = 2$). For convenience, we show the calculations for three species ($M = 3$). Nonetheless, for large number of species, one can follow the procedure given below. In this case, the systems' evolution is governed by the following equations [see Eqs. (1) and (2) in the main text]

$$\dot{n}_\sigma = n_\sigma \left[\sum_{i=1}^2 \alpha_{\sigma i} r_i(c_i) - \beta_\sigma - \epsilon_\sigma n_\sigma \right] \quad \sigma = 1, 2, 3, \quad (\text{S32})$$

$$\dot{c}_i = \mu_i(\Lambda_i - c_i) - r_i(c_i) \sum_{\sigma=1}^3 n_\sigma \alpha_{\sigma i} \quad i = 1, 2. \quad (\text{S33})$$

As discussed in the main text, the condition for all species to coexist is that the solutions $r_i(c_i^*)$ of the following equations [see Eq. (5) of the main text]:

$$r_1 \left[\frac{\alpha_{21}(r_1\alpha_{21} + r_2\alpha_{22} - \beta_2)}{\epsilon_2} + \frac{\alpha_{31}(r_1\alpha_{31} + r_2\alpha_{32} - \beta_3)}{\epsilon_3} - \frac{\beta_1\alpha_{11}}{\epsilon_1} + \frac{\alpha_{11}(r_1\alpha_{11} + r_2\alpha_{12})}{\epsilon_1} \right] = \mu \left(\Lambda_1 - \frac{r_1 k_1}{1 - r_1} \right), \quad (\text{S34})$$

$$r_2 \left[\frac{\alpha_{22}(r_1\alpha_{21} + r_2\alpha_{22} - \beta_2)}{\epsilon_2} + \frac{\alpha_{32}(r_1\alpha_{31} + r_2\alpha_{32} - \beta_3)}{\epsilon_3} - \frac{\beta_1\alpha_{12}}{\epsilon_1} + \frac{\alpha_{12}(r_1\alpha_{11} + r_2\alpha_{12})}{\epsilon_1} \right] = \mu \left(\Lambda_2 - \frac{r_2 k_2}{1 - r_2} \right), \quad (\text{S35})$$

should lie inside the region given by [see Eq. (6) of the main text]

$$\alpha_{11}r_1(c_1^*) + \alpha_{12}r_2(c_2^*) > \beta_1, \quad (\text{S36})$$

$$\alpha_{21}r_1(c_1^*) + \alpha_{22}r_2(c_2^*) > \beta_2, \quad (\text{S37})$$

$$\alpha_{31}r_1(c_1^*) + \alpha_{32}r_2(c_2^*) > \beta_3. \quad (\text{S38})$$

In Eqs. (S34) and (S35) we substitute $c_i^* = \frac{r_i k_i}{1 - r_i}$ (inverting the Monod function), and for convenience, we write $r_i = r_i(c_i^*)$

To gain a better insight, we first fix the parameters of the model $\beta_\sigma = 1$, $\mu = 0.001$, $k_i = 5$, $E = \text{diag}(0.001, 0.002, 0.003)$, and

$$Q = \begin{pmatrix} 1.5 & 2.8 \\ 3.1 & 5.2 \\ 1.7 & 2.5 \end{pmatrix}. \quad (\text{S39})$$

Notice that in the following, we consider Λ as a tuning parameter.

Now using Eqs. (S36)–(S38), we show the coexistence region where all initial species survive in Fig. S1(a). For given $\Lambda_1 = 3 \times 10^5$, we plot the equation of contour (S34) and for two different values of Λ_2 , i.e., (1) $\Lambda_2 = 10^6$ and (2) $\Lambda_2 = 10^5$, we plot Eq. (S35). For the first case (1), the solution of Eqs. (S34) and (S35) lies inside the shaded region whereas in the second case (2), it is outside of that region. Thus, for the first case (1), all the species coexist [see Fig. S1 (b)], whereas two species get extinct in Fig. S1 (c) referring to the second case (2). In Figs. S1 (b) and (c), the solid lines indicate the evolution of species while the dashed ones are for resources.

Finally, we emphasize that the above method is also applicable to predict the coexistence of any number of species competing for a large number of resources.

DERIVATION OF EQ. (7)

In this section we compute the exact probability density function, Eq. (7) of the main text, for the population sizes of M species when all of them survive, in the presence of one resource.

In this case, the population of M species is given by

$$n_\sigma^* = \frac{\alpha_\sigma r(c^*) - \beta_\sigma}{\epsilon_\sigma}, \quad (\text{S40})$$

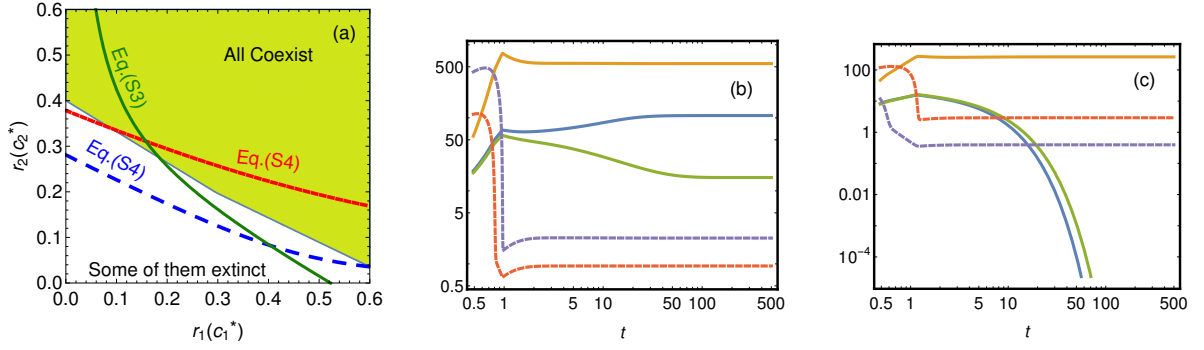


FIG. S1: Coexistence of three species in the presence of two resources. Panel (a): The shaded region is obtained from Eqs. (S36)–(S38). Eq. (S34) is plotted for $\Lambda_1 = 3 \times 10^5$ while Eq. (S35) is shown for two different Λ_2 , where for $\Lambda_2 = 10^6$ (red dashed line) the intersection (solution of Eqs. (S34) and (S35)) is inside the shaded region whereas for $\Lambda_2 = 10^5$ (blue dashed line), the solution is outside of shaded region. Panels (b) and (c): We numerically integrate the dynamics of the systems given in Eqs. (S32) and (S33) for given parameters for two different Λ_2 as discussed for Panel (a). In all plots, the parameters are $\beta_\sigma = 1$, $\mu = 0.001$, $k_i = 5$, $E = \text{diag}(0.001, 0.002, 0.003)$ and $\alpha_{\sigma i}$ is given by matrix Q in Eq. (S39). In Panel (b) and (c), the solid lines indicate the evolution of species population while the dashed ones are for resources.

where $r(c^*)$ is the solution of

$$Ar^2(c^*) - Br(c^*) - \mu(\Lambda - c^*) = 0, \quad (\text{S41})$$

in which coefficients $A = \sum_\sigma \alpha_\sigma^2 / \epsilon_\sigma$ and $B = \sum_\sigma \alpha_\sigma \beta_\sigma / \epsilon_\sigma$ depends only on the species characteristics.

Clearly, for given values of $\alpha_\sigma, \beta_\sigma, \epsilon_\sigma$ for all σ , $r(c^*)$ can be computed numerically using Eq. (S41) at fixed μ and Λ . Note that Λ is chosen such that all of the species have survived [see Fig. 1 in the main text].

In what follows, for simplicity, we fix $\beta_\sigma = 1$. Now given the distribution with which both α -s and ϵ -s are distributed, n -s are also distributed randomly, and we aim to obtain its distribution. In other words, α and ϵ are the random variables of which α_σ and ϵ_σ are the different realizations (i.e., independently drawn from their distributions). Since the random variable we are interested in is given by the ratio of two random variables, let us define $z = \frac{x}{y}$ [see Eq. (S40)], where $x = \alpha r(c^*) - 1$ and $y = \epsilon$. Thus, we have $z \in \{n_1^*, n_2^*, \dots, n_M^*\}$ whose distribution we want to find.

First we show the derivation for two scenarios discussed in main text: (1) $Q_2(\epsilon) = \delta(\epsilon - \hat{\epsilon})$ and (2) $Q_1(\alpha) = \delta(\alpha - \hat{\alpha})$. In the first case (1), we find that the population of the species is

$$z = \frac{x}{\hat{\epsilon}}. \quad (\text{S42})$$

Now using the Jacobian transform, one gets the distribution of z :

$$\begin{aligned} P(z) &= Q_1(\alpha) \left| \frac{d\alpha}{dx} \right| \left| \frac{dx}{dz} \right| \\ &= \frac{\hat{\epsilon}}{r(c^*)} Q_1\left(\frac{\hat{\epsilon}z + 1}{r(c^*)}\right), \end{aligned} \quad (\text{S43})$$

where $Q_1(\alpha)$ is the distribution with which α -s are distributed.

Similarly, for the second case (2), we have

$$z = \frac{\hat{\alpha}r(c^*) - 1}{y}, \quad (\text{S44})$$

where $y \in (\epsilon_1, \epsilon_2, \dots, \epsilon_M)$, i.e., distributed according to distribution $Q_2(y)$. Using again the Jacobian transform, we find

$$\begin{aligned} P(z) &= Q_2(y) \left| \frac{dy}{dz} \right| \\ &= \frac{\hat{\alpha}r(c^*) - 1}{z^2} Q_2\left(\frac{\hat{\alpha}r(c^*) - 1}{z}\right). \end{aligned} \quad (\text{S45})$$

In the case when both α -s and ϵ -s are distributed randomly, one can compute the distribution of $z = x/y$ as follows:

$$\begin{aligned} P(z) &= \int dx \int dy Q_1(x)Q_2(y) \delta\left(z - \frac{x}{y}\right), \\ &= \frac{1}{z^2} \int dx \int dy |x|Q_1(x)Q_2(y) \delta\left(y - \frac{x}{z}\right), \end{aligned} \quad (\text{S46})$$

where $Q_1(x) = Q_1(\alpha)|\frac{d\alpha}{dx}|$, and coming to the second equality from the first one, we have used the Jacobian transformation. In the above equation, the integrations are performed over the supports in which the distributions $Q_1(x)$ and $Q_2(y)$ are defined. We stress that above three scenarios are the exact results and can be used to compute the distribution of z for any given distributions $Q_1(x)$ and $Q_2(y)$.

In the following, for simplicity, we consider the case when α -s and ϵ -s are distributed uniformly such that $\alpha \in (a, b)$ and $\epsilon \in (c, d)$. Therefore, we find $x \in (p, q)$ in which $p \equiv a r(c^*) - 1$ and $q \equiv b r(c^*) - 1$ (where $0 < p < q$ since we assumed all the species survive), and $y \in (c, d)$.

Therefore, the probability density function of the population is

$$\begin{aligned} P(z) &= \frac{1}{(q-p)(d-c)z^2} \int_p^q dx |x| \overbrace{[\Theta(x-p) - \Theta(x-q)]}^{=1 \text{ since } 0 < p < q} [\Theta(x/z - c) - \Theta(x/z - d)] \\ &= \frac{1}{(q-p)(d-c)z^2} \int_p^q dx \overbrace{|x|}^x [\Theta(x/z - c) - \Theta(x/z - d)], \end{aligned} \quad (\text{S47})$$

where $\Theta(\cdot)$ is the Heaviside theta function.

Now we replace x/z by t and find

$$\begin{aligned} P(z) &= \frac{1}{(q-p)(d-c)} \int_{p/z}^{q/z} dt t [\Theta(t - c) - \Theta(t - d)] \\ &= \frac{1}{(q-p)(d-c)} [I_1(c, z) - I_1(d, z)]. \end{aligned} \quad (\text{S48})$$

Finally, solving the following integral, we get

$$I_1(\kappa, z) = \int_{p/z}^{q/z} dt t [\Theta(t - \kappa)] = \begin{cases} 0 & \kappa > q/z, \\ \frac{1}{2z^2}(q^2 - \kappa^2 z^2) & p/z < \kappa < q/z, \\ \frac{1}{2z^2}(q^2 - p^2) & \kappa < p/z < q/z, \end{cases} \quad (\text{S49})$$

and substituting it in Eq. (S48), we obtain Eq. (7) of the main text:

$$P(z) = \frac{1}{2z^2(q-p)(d-c)} [J_1(c, z) - J_1(d, z)], \quad (\text{S50})$$

where $J_1(\kappa, z) = 2z^2 I_1(\kappa, z)$.

CALCULATION FOR Λ_l IN THE PRESENCE OF ONE RESOURCE

In this section we compute the critical value of Λ , i.e., Λ_l , for l number of surviving species starting from $M \geq l$ species.

We note that when Λ is less than the threshold $\bar{\Lambda}$ [see Fig. 1 of the main text], some species start going extinct with time. Moreover, the number of the extinct species depends on the choice of Λ once all the other parameters are fixed. In this case, we find the stationary state from Eqs. (S32) and (S33) ($\beta_\sigma = 1$)

$$n_\sigma^* = \frac{\alpha_\sigma \tilde{r}(c^*) - 1}{\epsilon_\sigma} U(\alpha_\sigma - \bar{\alpha}) \quad (\text{S51})$$

$$\tilde{r}(c^*) = \frac{\mu(\Lambda - c^*)}{\sum_\sigma n_\sigma^* \alpha_\sigma}. \quad (\text{S52})$$

Note that sum in the (S52) is restricted because some n_σ -s are equal to zero (when $\alpha_\sigma < \tilde{\alpha}$) as shown in (S51). Also the number $\tilde{\alpha}$ is yet to obtain. In the above Eq. (S51) $U(x)$ is the Unit-step function with $U(x \geq 0) = 1$ and 0 otherwise.

Substituting Eq. (S51) in Eq. (S52), we find

$$\tilde{A}\tilde{r}^2(c^*) - \tilde{B}\tilde{r}(c^*) - \mu(\Lambda - c^*) = 0, \quad (\text{S53})$$

where $\tilde{A} = \sum_\sigma \frac{\alpha_\sigma^2}{\epsilon_\sigma}$ and $\tilde{B} = \sum_\sigma \frac{\alpha_\sigma}{\epsilon_\sigma} U(\alpha_\sigma - \tilde{\alpha})$.

Thus, the fraction of surviving species can be obtained as

$$f_s = \frac{1}{M} \sum_{\sigma=1}^M U(\alpha_\sigma - \tilde{\alpha}), \quad (\text{S54})$$

where the fraction of extincted ones is $f_e = 1 - f_s$.

In the following, we aim to obtain the cut-off $\tilde{\alpha}$. This depends on the value of Λ and the choice of α -s and ϵ -s. To do so, we first define $A_l^{(c)}$ and $B_l^{(c)}$, where

$$A_l^{(c)} = \sum_{j=1}^l \frac{\alpha_j^2}{\epsilon_j}, \quad (\text{S55})$$

$$B_l^{(c)} = \sum_{j=1}^l \frac{\alpha_j}{\epsilon_j}, \quad (\text{S56})$$

in which $1 \leq l \leq M$. Note that the above sum is performed over the species that are arranged in descending order in α : $\{\alpha_1, \epsilon_1; \alpha_2, \epsilon_2; \dots; \alpha_M, \epsilon_M\}$, where the species with highest α has parameters α_1 and ϵ_1 .

Now if l number of species survive starting from M , we find from Eq. (S51) that

$$\begin{aligned} \tilde{r}(c^*) &> \alpha_l^{-1} \\ &= \tilde{r}(\bar{c}) = \max\{\alpha_\sigma^{-1} \mid 1 \leq \sigma \leq l\}. \end{aligned} \quad (\text{S57})$$

and we define the critical supply for first l species to survive

$$\Lambda_l = \frac{\tilde{r}(\bar{c})}{\mu} \left[A_l^{(c)} \tilde{r}(\bar{c}) - B_l^{(c)} \right] + \frac{k\tilde{r}(\bar{c})}{1 - \tilde{r}(\bar{c})}. \quad (\text{S58})$$

Thus, given the above solution, we can systematically evaluate the value of l for which $\Lambda_l < \Lambda < \Lambda_{l+1}$, and therefore, we can easily infer the cut-off $\tilde{\alpha} = \alpha_l$. Similarly, this can also be useful to predict the total number of surviving species and is shown in Fig. 2(a) of the main text.

DERIVATION OF EQ. (8)

In this section we compute the distribution of population sizes for surviving species starting from a pool M species at a large-time. Here again, we consider the case when both α and ϵ are distributed uniformly.

Now the range of the numerator of (S51) is $p = 0$, $q = b\tilde{r}(c^*) - 1$ where $\tilde{r}(c^*)$ is the solution of Eq. (S53).

Thus, the probability distribution of population sizes of the coexisting species is given by

$$\begin{aligned} P(z) &= \int_0^q dx \int_c^d dy Q_1(x) Q_2(y) \delta\left(z - \frac{x}{y}\right) \\ &= \frac{1}{q(d-c)} \int_0^q dx \int_c^d dy [\Theta(x) - \Theta(x-q)][\Theta(y-c) - \Theta(y-d)] \delta\left(z - \frac{x}{y}\right) \\ &= \frac{1}{q(d-c)z^2} \int_0^q dx |x| \overbrace{[\Theta(x) - \Theta(x-q)]}^{=1 \text{ since } 0 < q} [\Theta(x/z-c) - \Theta(x/z-d)] \\ &= \frac{1}{q(d-c)z^2} \int_0^q dx \overbrace{|x|}^x [\Theta(x/z-c) - \Theta(x/z-d)]. \end{aligned} \quad (\text{S59})$$

Finally, we replace x/z by t and get

$$P(z) = \frac{1}{q(d-c)} [I_2(c, z) - I_2(d, z)], \quad \text{where} \quad (\text{S60})$$

$$I_2(\kappa, z) = \int_0^{q/z} dt t[\Theta(t - \kappa)] = \begin{cases} 0 & \kappa > q/z, \\ \frac{1}{2z^2}(q^2 - \kappa^2 z^2) & 0 < \kappa < q/z, \end{cases} \quad (\text{S61})$$

which gives Eq. (8) in the main text by substituting $J_2(\kappa, z) = 2z^2 I_2(\kappa, z)$.

THE POPULATION DISTRIBUTION FOR LARGE NUMBER OF RESOURCES

In this section, we compute the distribution of population of species when the number of resources are very large $R \gg 1$. For large number of resources, it is difficult to obtain the exact distribution for the population. Nonetheless, it is possible to obtain the approximate distribution.

In this case, the equation for the non-zero population sizes of M^* surviving species (in the stationary state) can be obtained from Eq. (S32):

$$n_\rho^* = \frac{1}{\epsilon_\rho} \left(\sum_{i=1}^R \alpha_{\rho i} r_i(c_i^*) - 1 \right), \quad (\text{S62})$$

where $1 \leq \rho \leq M^*$ are the species with non-zero population.

In the above Eq. (S62), we have to first find the distribution according to which the numerator is distributed. We again stress that once $\alpha_{\rho i}$ are drawn, $r_i(c_i^*)$ -s are fixed numbers that only depend on the surviving species ($n_\rho^* > 0$).

Let us first discuss the numerator of the above equation. We define $w = h - 1$, where

$$h = \sum_{j=1}^R x_j a_j. \quad (\text{S63})$$

We can write the mean and the variance of x_j , respectively, as $\theta = \langle x_j \rangle$ and $\phi^2 = \langle x_j^2 \rangle - \theta^2$ in which the angular brackets represent the average with respect to the distribution with which α -s are distributed. Herein, x_j -s and a_j , respectively, play the role of $\alpha_{\rho i}$ and $r_i(c_i)$ for a given ρ .

The mean of $\langle h \rangle = \theta \sum_j a_j$ [see Eq. (S63)]. Therefore, the quantity $v = \sum_j a_j (x_j - \theta)$ has zero mean and zero variance given by

$$\begin{aligned} \langle v^2 \rangle &= \sum_j a_j^2 \langle (x_j - \theta)^2 \rangle + \sum_{i \neq j} a_i a_j \langle (x_i - \theta)(x_j - \theta) \rangle \\ &= \sum_j a_j^2 \langle (x_j - \theta)^2 \rangle + \sum_{i \neq j} a_i a_j \langle x_i x_j + \theta^2 - \theta x_j - \theta x_i \rangle, \\ &= \phi^2 \sum_j a_j^2, \end{aligned} \quad (\text{S64})$$

where the last term in the second equality is zero since x_i -s are independent.

Now, we define the rescaled sum as

$$S = \sum_j b_j m_j, \quad (\text{S65})$$

where $b_j = \frac{a_j}{\sqrt{\sum_j a_j^2}}$, and $m_j = (x_j - \theta)/\phi$. In the following, we also assume that $b_j \sim 1/\sqrt{R}$.

Now the probability density function for S is

$$\begin{aligned}
P_1(S) &= \frac{1}{2\pi} \int dk e^{ikS} \prod_{j=1}^R \left(\int dm_j e^{-ikb_j m_j} p(m_j) \right) \\
&= \frac{1}{2\pi} \int dk e^{ikS} \prod_{j=1}^R \langle e^{-ikb_j m_j} \rangle \\
&\approx \frac{1}{2\pi} \int dk e^{ikS} \prod_{j=1}^R \left[1 - k^2 \frac{b_j^2}{2} + \dots \right] \\
&\approx \frac{1}{2\pi} \int dk e^{ikS} \left[1 - k^2 \frac{\sum_{j=1}^R b_j^2}{2} + \dots \right] \\
&\approx \frac{1}{2\pi} \int dk e^{ikS} e^{-k^2/2} \\
&\approx \frac{1}{\sqrt{2\pi}} e^{-\frac{S^2}{2}}, \tag{S66}
\end{aligned}$$

where $\sum_j b_j^2 = 1$, and each m has zero and unit variance, and also $R \gg 1$.

Since $h = S\phi\sqrt{\sum_j a_j^2} + \theta\sum_j a_j$, the probability density function for z is

$$p_1(h) \approx \frac{1}{\sqrt{2\pi(\sum_j a_j^2)\phi^2}} \exp \left[-\frac{(h - \theta\sum_j a_j)^2}{2(\sum_j a_j^2)\phi^2} \right] \tag{S67}$$

Therefore,

$$p_2(w) \approx \frac{1}{\sqrt{2\pi(\sum_j a_j^2)\phi^2}} \exp \left[-\frac{[w - (\theta\sum_j a_j - 1)]^2}{2(\sum_j a_j^2)\phi^2} \right]. \tag{S68}$$

Thus, the numerator of (S62) is typically distributed according to the above shown Gaussian distribution. In Fig. S2 (a), we compare the distribution given in Eq. (S68) with proper rescaling where the rescaled variable is $\xi = \frac{w - \langle w \rangle}{\sqrt{\text{Var}[w]}}$, with the numerical simulation of the dynamics given in Eqs. (S32) and (S33), where the solid curve is the analytical prediction and the circles are obtained from numerical simulation. We can see that there is a good agreement between theory and numerical simulation.

Now, we aim to find the ratio $z = w/y$ assuming the denominator to be uniformly distributed such that $y \in \mathcal{U}(c, d)$ this distribution, we have

$$\begin{aligned}
P(z) &= \int dw \int dy p_2(w) Q_2(y) \delta\left(z - \frac{w}{y}\right) \\
&= \frac{1}{z^2} \int dw \int dy |w| p_2(w) Q_2(y) \delta\left(y - \frac{w}{z}\right) \\
&\approx \frac{1}{z^2 \sqrt{2\pi\Sigma^2}} \int_{-\infty}^{\infty} dw |w| \exp \left[-\frac{(w - \mathcal{M})^2}{2\Sigma^2} \right] Q_2(w/z) \\
&\approx \frac{1}{\sqrt{2\pi\Sigma^2}} \int_{-\infty}^{\infty} dt |t| \exp \left[-z^2 \frac{(t - \mathcal{M}/z)^2}{2\Sigma^2} \right] [\Theta(t - c) - \Theta(t - d)] \\
&\approx \frac{1}{(d - c)\sqrt{2\pi\Sigma^2}} \int_c^d dt t \exp \left[-z^2 \frac{(t - \mathcal{M}/z)^2}{2\Sigma^2} \right] \\
&\approx \frac{1}{\sqrt{2\pi}(d - c)z^2} \left[\Sigma \left(e^{-\frac{(\mathcal{M} - cz)^2}{2\Sigma^2}} - e^{-\frac{(\mathcal{M} - dz)^2}{2\Sigma^2}} \right) \right. \\
&\quad \left. + \sqrt{\frac{\pi}{2}} \mathcal{M} \left\{ \text{Erf} \left(\frac{\mathcal{M} - cz}{\sqrt{2}\Sigma} \right) - \text{Erf} \left(\frac{\mathcal{M} - dz}{\sqrt{2}\Sigma} \right) \right\} \right], \tag{S69}
\end{aligned}$$

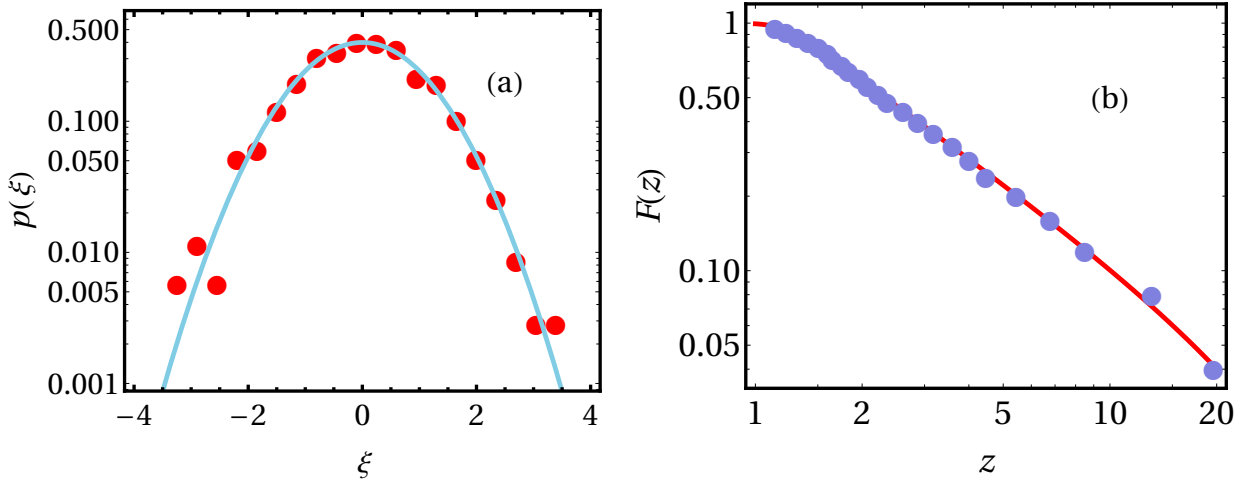


FIG. S2: Species in the presence of large number of resources. Panel (a): We numerically verified the Gaussian distribution given in Eq. (S68) with proper rescaling where the rescaled variable $\xi = \frac{w-(w)}{\sqrt{\text{Var}[w]}}$. The solid curve is given by $p(\xi) = \frac{1}{\sqrt{2\pi}} \exp(-\xi^2/2)$ whereas the circles are obtained by numerically simulating the dynamics given in Eqs. (1) and (2) in the main text. Panel (b): We compare the complementary cumulative function obtained from the analytical distribution given in Eq. (S69) with the numerical simulation of the dynamics. We can see that there is a good agreement between theory and numerical simulation. For both panels, we consider $M = 1000$, $R = 50$, $\mu = 0.001$, $k = 5$, $\alpha \in \mathcal{U}(1.5, 5.0)$, $\epsilon \in \mathcal{U}(0.01, 0.5)$, $\beta_\sigma = 1$, $\Lambda_i = 1.5 \times 10^5$ for all i , and $t = 10^{50}$.

where $\mathcal{M} = \theta \sum_j a_j - 1$ and $\Sigma = \sqrt{\phi^2 \sum_j a_j^2}$. Here $\theta = \int d\alpha p(\alpha) \alpha$, $\phi^2 = \int d\alpha p(\alpha) (\alpha - \theta)^2$, and $a_j = r_j(c_j^*)$.

In Fig. S2(b), we compare the above Eq. (S69) with the numerical simulation of the dynamics given in Eqs. (S32) and (S33), where the solid curve is the analytical prediction and the circles are obtained from numerical simulation. Finally, we stress that in this case, either exact or numerical value of $r_i(c_i^*)$ is difficult to obtain. Therefore, we have taken $r_i(c_i^*)$ from the numerical simulation of the dynamics the dynamics given in Eqs. (1) and (2) in the main text.

POWER-LAW EXPONENTS FOR DATA

In this section, we present an analysis on our model [see Eqs. (1) and (2) in the main text], to show it predicts fat-tail probability distribution for the population size. Herein, we show how power-law tails can be observed with a possible the range of variability of the exponent. We remark that this calculation will predict the tails of the empirical distribution of the Plankton data shown in the main text.

We recall the ratio $z = \frac{x}{y}$ and its distribution is given by [see Eq. (S46)]

$$P(z) = \frac{1}{z^2} \int dx \int dy |x| Q_1(x) Q_2(y) \delta\left(y - \frac{x}{z}\right). \quad (\text{S70})$$

We have already shown above when x and y are uniformly distributed, the distribution of z has a power-law tail with exponent -2 [see Eqs. (S50) and (S60)]. We also showed that when species are competing for a relatively large number of resources $R \gg 1$, we again observe a power-law with an exponent -2 [see Eq. (S69)] under the assumption that ϵ are uniformly distributed. In the following, we show that our extended consumer-resource model could retrieve a range of exponents for the power-law tail of the distribution. In order to make things transparent, let us begin our analysis from a simple setting: $Q_1(x) = \delta(x - \hat{x})$. Hence Eq. (S70) reduces to

$$P(z) = \frac{\hat{x}}{z^2} Q_2(\hat{x}/z) [\Theta(\hat{x} - zy_-) - \Theta(\hat{x} - zy_+)], \quad (\text{S71})$$

where we have assumed that the random variable y takes values in the interval $[y_-, y_+]$ (consequently $z \in \left[\frac{\hat{x}}{y_+}, \frac{\hat{x}}{y_-}\right]$). Suppose the distribution $Q_2(y)$ is

$$Q_2(y) = \frac{N}{y^\nu}, \quad (\text{S72})$$

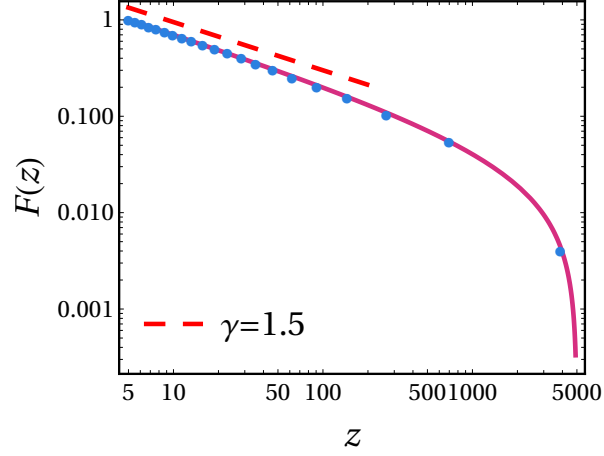


FIG. S3: Comparison of analytical result (S75) with the numerical simulation. The solid curve is theoretical prediction of the complementary cumulative distribution $F(z) = \int_z^\infty dy P(y)$ obtained from Eq. (S75), while the blue dots are obtained numerically after having sampled $M = 10^4$ independent draws from the distribution Eq. (S72). The parameters for the plot are $\hat{x} = 5$, $y_- = 10^{-3}$, $y_+ = 1$ and $\nu = 0.5$. Clearly, we can see that there is an excellent match. In the plot, the dashed line is indicated for $F(z) \sim z^{-\gamma+1}$, where $\gamma = 1.5$. We remark that the deviation at a large z from the power-law is due to presence of Heaviside functions in the prefactor of Eq. (S74), that introduce cut-off effects.

where the normalization constant N is given by

$$1 = \frac{N}{1 - \nu} [y^{-\nu+1}] \Big|_{y_-}^{y_+}. \quad (\text{S73})$$

Since we would like to deal with small y (i.e., small ϵ that gives large carrying capacity) we can consider the limit $y_- \rightarrow 0$. In this limit N diverges if $\nu \geq 1$. Therefore, we must consider $\nu < 1$. Moreover, on a physical ground, we expect the probability density function of y (or ϵ) to decrease monotonically as y increases. This is because of the fact that a large number of species might have a small value of ϵ (or y) that results in a large carrying capacity for those species. Thus, under such assumption, we get $0 \leq \nu < 1$. Therefore, Eq. (S71) becomes

$$P(z) = \frac{B}{z^{2-\nu}} [\Theta(\hat{x}/y_- - z) - \Theta(\hat{x}/y_+ - z)]. \quad (\text{S74})$$

where $B = N\hat{x}^{1-\nu}$. Notice that the first Heaviside function gives the largest value of z above which the distribution vanishes. Therefore, we find that the distribution $P(z)$ is a power-law (with a prefactor):

$$P(z) \sim z^{-\gamma}. \quad (\text{S75})$$

where $\gamma = 2 - \nu \in (1, 2]$. We stress that $\nu = 0$ corresponds to the uniform distribution that we have considered in the previous sections. In Fig. S3, we show the comparison of the complementary cumulative distribution function $F(z) = \int_z^\infty dy P(y)$ obtained from Eq. (S75) with the numerical simulation (see caption of Fig. S3 for details).

We can extend this result to a broad class of distributions $Q_1(x)$ and $Q_2(y)$ using asymptotic analysis. Let us assume $y \in (0, y_+]$ and $x \in (0, x_+)$. This implies that $z \in (0, \infty)$. From Eq. (S70) we have that

$$P(z) = \frac{1}{z^2} \int_0^{\min\{x_+, zy_+\}} dx x Q_1(x) Q_2(x/z). \quad (\text{S76})$$

At this point we can distinguish two cases:

1. $Q_2(y)$ is regular at $y = 0$ with

$$\left. \frac{d^i}{dy^i} Q_2(y) \right|_{y=0} = 0 \quad \text{for } i = 0, \dots, n-1. \quad (\text{S77})$$

Then, in the limit of large z we write the following expansion:

$$Q_2\left(\frac{x}{z}\right) = \frac{x^n}{z^n} Q_2^{(n)}(0) + o\left(\frac{1}{z^n}\right). \quad (\text{S78})$$

Finally, we find

$$P(z) \sim \frac{1}{z^{2+n}} \overbrace{\left(Q_2^{(n)}(0) \int_0^{x^+} dx x^{1+n} Q_1(x) \right)}^{<\infty}. \quad (\text{S79})$$

2. $Q_2(y)$ diverges at $y = 0$ like a power-law, i.e., $Q_2(y) = \frac{A}{y^\nu}$ with $\nu \in [0, 1)$. Therefore, we have $(\frac{x}{z} \rightarrow 0 \text{ as } z \rightarrow \infty)$

$$P(z) \sim \frac{1}{z^{2-\nu}} \overbrace{\left(A \int_0^{x^+} dx x^{1-\nu} Q_1(x) \right)}^{<\infty}, \quad (\text{S80})$$

where in both Eqs. (S79) and (S80), the prefactors remain finite.

In all cases, the distribution $P(z)$ displays asymptotically a power-law tail, i.e.,

$$P(z) \sim \frac{1}{z^\gamma} \quad \text{for large } z, \quad (\text{S81})$$

with $\gamma \geq 2$ in the first case and $1 < \gamma \leq 2$ in the second one.

From an ecological point of view, the relevant case is the second one. Hence, the analysis we performed here indicates that the model presented in the main text predicts distributions of population size with power-law tails whose exponents ranges in an interval that we have shown above. In Figure S4, we show the comparisons of the theoretical results for two concrete examples, [one for each case, see Eqs. (S79) and (S80)] with the corresponding numerical simulations (see caption of Fig. S4 for more details), and clearly, they have a nice agreement.

DISCUSSION ON Figs. 2(a) AND 3(a-b)

In this section, we give the details on the simulation for $R > 1$ shown in Figs. 2(a) and 3(a-b) in the main text. As already mentioned in the main text that we can compute the exact curve for surviving species when these are competing one resource. However, such exact computation for $R > 1$ is not illuminating for us. Nevertheless, one can count the number of surviving species for a given Λ_i , where $1 \leq i \leq R$ by numerically integrating Eqs. (1) and (2) of the main text.

To compare the result for $R = 1$ and $R > 1$, we do a slight modification in our model, where we consider that all resources have same supply, i.e., $\Lambda_i = \Lambda$ for all i . Further, we assume that the metabolic strategies $\alpha_{\sigma i} = \alpha_\sigma q_i$, where $q_i \in \mathcal{U}[0, 1]$ is a resource dependent uniform random variable such that $\sum_i q_i = 1$. Using this, Eqs. (1) and (2) can be rewritten as follows:

$$\dot{n}_\sigma = n_\sigma \left[\alpha_\sigma \sum_{i=1}^R q_i r_i(c_i) - \beta_\sigma - \epsilon_\sigma n_\sigma \right], \quad (\text{S82})$$

$$\dot{c}_i = \mu_i(\Lambda - c_i) - r_i(c_i) q_i \sum_{\sigma=1}^M \alpha_\sigma n_\sigma, \quad (\text{S83})$$

where M and R , respectively, are the number of species and resources. For convenience, we set $\mu_i = \mu$ and $\beta_\sigma = 1$ (same as in main text). Now we fix α_σ for M species, and numerically integrate the coupled dynamics (S82) and (S83), and count the number of species surviving as a function for Λ for different number of resources and this result is shown in Fig. 2(a) of the main text.

Similarly, we compute the distribution of the population in Figs. 3(a-b) of the main text for different resources. As we can see from Fig. 2(a) (main text) that when Λ is sufficiently large, all initial species survives. In that case, the population of the species in the stationary state can be written using Eq. (S82):

$$n_\sigma^* = \frac{\alpha_\sigma \sum_i q_i r_i(c_i^*) - 1}{\epsilon_\sigma}. \quad (\text{S84})$$

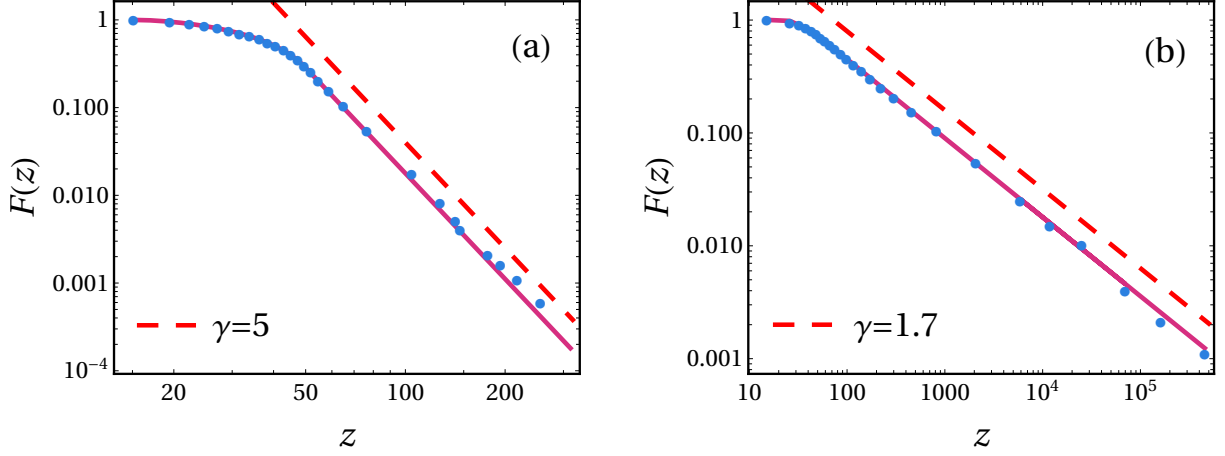


FIG. S4: Comparison of theoretical prediction of Eqs. (S79) and (S80) with the numerical simulations. The solid curves are the theoretical prediction of the complementary cumulative distribution $F(z) = \int_z^\infty dy P(y)$ obtained from Eq. (S79) [for panel (a)] and Eq. (S80) [for panel (b)], while blue dots are obtained from numerical simulation in which we generated $M = 10^4$ independent draws for the numerator and denominator by sampling the respective probability distributions (details are given below). Panel (a): We consider the case in which the denominator of the ratio $z = x/y$ is distributed according to a regular function at $y = 0$. In concrete, we take $Q_2(y) = Cy^3$ in the interval $[0, 0.1]$ (C is the normalization constant) while the numerator is assumed to be uniformly distributed in the interval $[1.5, 5]$, i.e., $Q_1(x) = \mathcal{U}(1.5, 5)$. Panel (b): $Q_2(y)$ is chosen to be a power-law distribution with exponent $\nu = 0.3$ on the same interval $[0, 0.1]$ while the numerator is again distributed uniformly in the interval $[1.5, 5]$. As expected, a power-law for large- z is observed. In both panels, we plot the dashed line corresponding to $F(z) \sim z^{-\gamma+1}$, where $\gamma = 5$ for panel (a) and for panel (b), we find $\gamma = 1.7$ as predicted by the theoretical investigation in Eqs. (S79) and (S80).

We have checked numerically that when Λ is very large, $r_i(c_i^*) \rightarrow 1$. In that case,

$$n_\sigma^* \approx \frac{\alpha_\sigma - 1}{\epsilon_\sigma}, \quad (\text{S85})$$

since $\sum_i q_i = 1$. Therefore, the distribution of the population is independent of the number of resources, and in the case when α and ϵ are distributed uniformly, the distribution is given by Eq. (S50). In Fig. S5, we show the comparison of the numerical simulation for different number of resources for $\Lambda = 10^{12}$ [see Fig. 2(a) in the main text] and the analytical prediction given in Eq. (S50), and we find an excellent match between them.

DISCUSSION ON Fig. 2(b)

Fig. S6 shows the explicit observations we discussed for Fig. 2(b) of the main text. For this figure, the other parameters are $\beta_1 = \beta_2 = \beta_3 = 1$, $\epsilon_1 = 0.0015$, $\epsilon_2 = 0.0025$, $\epsilon_3 = 0.0017$, $k = 5$, $\mu = 0.001$, and $\Lambda = 10^6$. In the end, we stress that it is not mandatory for the initial two species (circle and star) to reach a stationary state and then invader arrive. Even if the system of these two species does not reach stationary state and the invader participate in the competition, the results do not change.

PARAMETERS FOR FIGURES IN MAIN TEXT

1. Fig. 1: $M = 4$, $R = 1$, $k = 5$, $\beta = 1$, $\mu = 0.001$, $\vec{\alpha} = (4.3, 2.5, 3.8, 4.7)$, $\vec{\epsilon} = (0.003, 0.00258, 0.00175, 0.00454)$.
2. Figs. 2(a), and 3(a-b): $M = 500$, $\alpha_\sigma \in \mathcal{U}(1.5, 10.0)$, $\beta_\sigma = 1$, $\mu = 0.001$, $\epsilon_\sigma \in \mathcal{U}(0.0001, 0.0005)$, $k_i = 5$. For Fig. 3(a), $\Lambda = 3 \times 10^{10}$ and for Fig. 3(b), $\Lambda = 5 \times 10^8$ [see Fig. 2(a)].

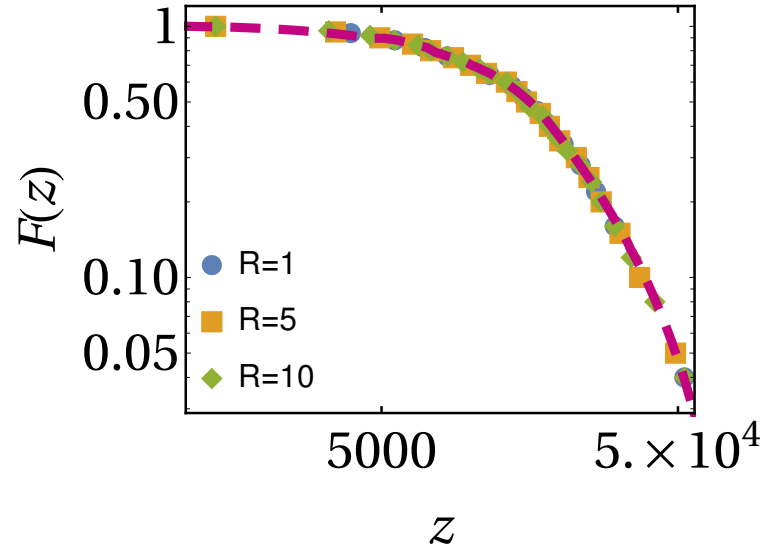


FIG. S5: CCDF for the population sizes of 500 species competing for 1, 5, and 10 resources. The symbols are obtained from numerically integrating Eqs. (S82) and (S83). The solid line is the analytical result for $R = 1$ given in Eq. (S50). Clearly, we can see that there is no dependence on the number of resources. Other parameters are $\alpha_\sigma \in \mathcal{U}(1.5, 10.0)$, $\beta_\sigma = 1$, $\mu = 0.001$, $\epsilon_\sigma \in \mathcal{U}(0.0001, 0.0005)$, $k_i = 5$, and $\Lambda = 10^{12}$.

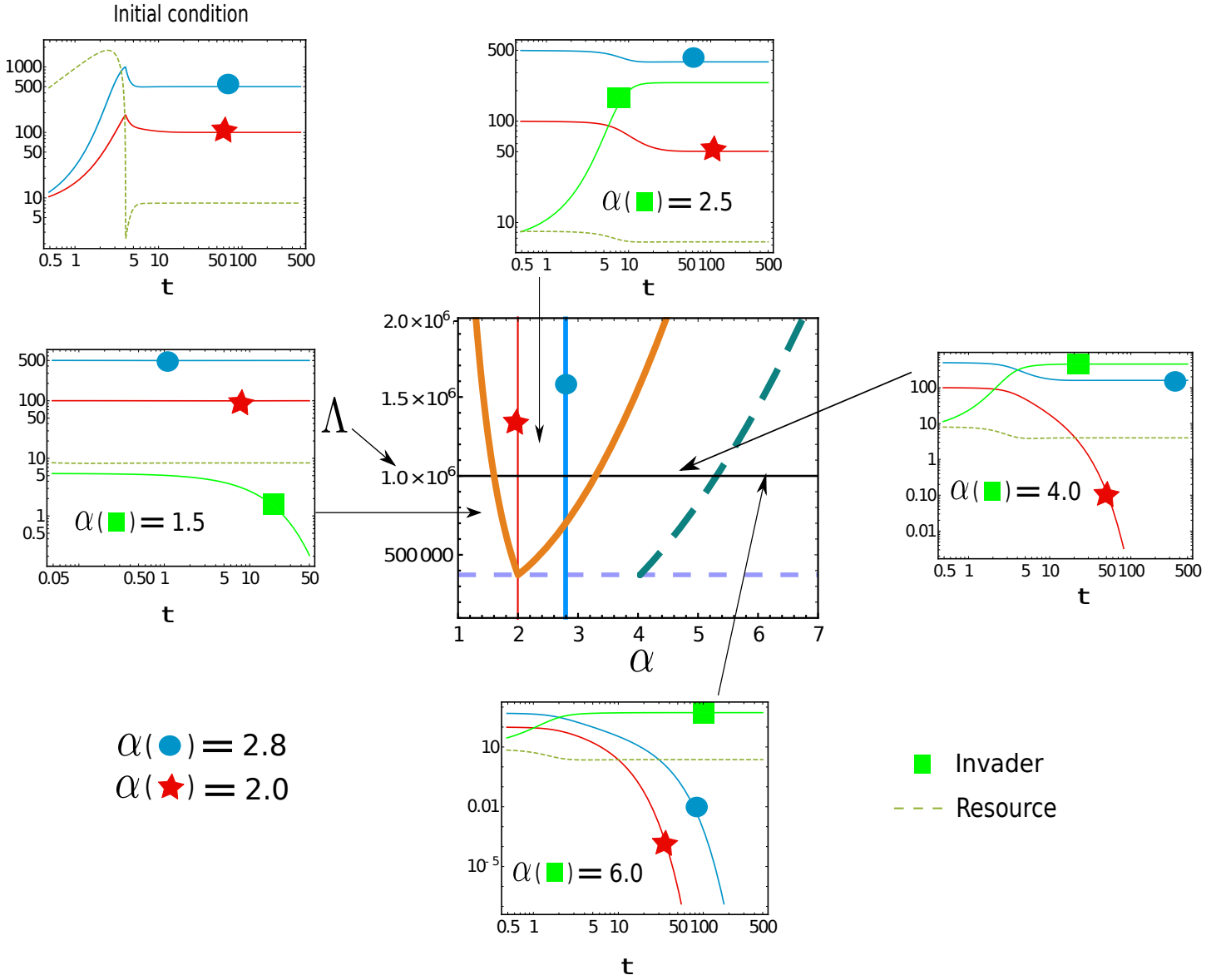


FIG. S6: Discussion on Fig. 2(b) of the main text. We begin (see top left corner) with two species (star and circle) at a given Λ (solid horizontal black line) greater than the dashed line (critical value for both these species to survive). Once the system reaches steady state, an invader arrives (shown by square), depending on its metabolic strategies, four possibilities can be seen and those are displayed in the central figure (similar to Fig. 2(b) of the main text). In the central figure, the solid orange curve indicates critical resource supply $\bar{\Lambda}$ for all three species to survive, and dashed green curve (right side) is the critical resource supply $\bar{\Lambda}$ for invader and circle to survive. As discussed in Fig. 2(b) of the main text, we can verify that there are four regions depending what are the species survive in these regions. Note that the clock is restarted from zero (for convenience) when all three species start interacting.